As part of the study of SGHW lattices at AEE Winfrith, a wide range of uniform cluster arrays has been studied. Both enriched $UO_2$ and $PuO_2/UO_2$ fuels have been used and the range includes pin diameters from 0.3 in to 0.5 in in clusters containing from 37 to 90 pins each. Measurements of material buckling, detailed reaction rates and void coefficient have been compared with theoretical predictions using METHUSELAH II, which is an improved version of the five-group diffusion theory code, METHUSELAH I, originally developed for SGHW assessment and design studies, and the 69-group, transport theory code, WIMS, which has now superseded THULE.

# Further reactor physics studies for steam generating heavy water reactors

## Part 1: Uniform cluster lattices containing $UO_2$ or $PuO_2/UO_2$ fuel

A. J. Briggs, BA*

I. Johnstone, BSc†

P. B. Kemshell, BSc*

D. A. Newmarch, BA, BSc*

### INTRODUCTION

A 100 MW(E) prototype Steam Generating Heavy Water (SGHW) Reactor, which has been described in detail elsewhere,[1, 2] will be brought into operation at AEE Winfrith during 1967. The fuel assemblies take the form of 36-pin clusters of low enrichment uranium oxide, clad in Zircaloy-2 and cooled by pressurized boiling light water. Each cluster is housed in a Zircaloy-2 pressure tube surrounded by a gas gap for thermal insulation and an aluminium alloy calandria tube. In addition to the standard boiling channels, there are a large number of non-standard experimental boiling channels and eight superheat channels. Unpressurized heavy water moderator fills the spaces between the calandria tubes except for the volume occupied by 74 aluminium moderator displacement tubes in interstitial positions. These tubes can be either empty or full of $D_2O$ and it is therefore possible to change the degree of undermoderation of the lattice and hence the local void coefficient and power distribution.

2. During the period 1961–67, an extensive programme of experimental and theoretical physics has been undertaken at Winfrith in support of the prototype project. This work is now largely completed and it is proposed to describe it in a series of reports of which this is the first. The titles of the various reports are as follows:

Part 1: Uniform cluster lattices containing $UO_2$ or $PuO_2/UO_2$ fuel

Part 2: Multi-zone cores for fuel management studies

Part 3: Coolant temperature effects in $UO_2$ and $PuO_2/UO_2$ fuels

Part 4: The study of a mock-up of the SGHW prototype in DIMPLE.

3. Early measurements made in uniform cluster lattices up to mid-1964 were first reported[3] at the 3rd International Conference on the Peaceful Uses of Atomic Energy at Geneva in 1964, and a more detailed comparison of the results with theoretical predictions was published as a separate report.[4] The measurements consisted of complete sets of detailed reaction rates with material buckling determinations to check neutron leakage and the self-consistency of the reaction rate measurements. The possible existence of systematic errors in these measurements was investigated in some detail[5] and it was shown that although the reaction rate measurements were, in general, satisfactory, the presence of cluster grids between the discontinuous fuel elements used in these early experiments led to significant uncertainties in the determination of material buckling in the critical cores. The range of uniform cluster lattices has now been augmented by the study of a number of $UO_2$ and $PuO_2/UO_2$ fuels, all of which are provided in continuous lengths and thus avoid the need for significant cluster grids.

4. The experimental techniques used for the reaction rate measurements up to 1964 were described in references 6 to 10. Further development of these techniques has taken

* General Reactor Physics Division, UKAEA, AEE, Winfrith.
† Group Leader, Project Experimental Physics Group, General Reactor Physics Division, UKAEA, AEE, Winfrith.

place in recent years, resulting in improved accuracy and requiring some minor changes in the values previously published, e.g. in the calibration of fast fission ratio determinations.

5. In the paper[3] presented at Geneva, the experimental results were compared with theoretical predictions using the five-group diffusion theory code METHUSELAH[11] and the 45-group transport code THULE.[12] METHUSELAH has now been written in an improved form, METHUSELAH II[13], which largely removes the defects which were shown in reference 4 to be present in the earlier version. THULE has been superseded by the Winfrith Improved Multi-group code WIMS, which has recently been described in detail in the literature.[14] Brief descriptions of important features of METHUSELAH II and WIMS are given below and the codes are then used to provide calculated values for comparison with each of the measured quantities. To conserve space in this journal, only the cluster average values of the various parameters are discussed in detail, although typical cluster distributions are also compared with theoretical predictions. For those wishing to compare measured and predicted flux and reaction rate distributions across the lattice cell, the necessary details are provided in references 15 and 16.

## THE EXPERIMENTAL PROGRAMME

### Aims of programme

The study of uniform cluster SGHW lattices was carried out during the period 1961–65. The earlier work was concerned with enriched uranium fuelling only and had the following aims:

(i) to confirm reactivity calculations for SGHW lattices to within ±1%;

(ii) to provide experimental confirmation of methods of predicting cluster power peaking to within ±5%;

(iii) to measure the void coefficient in a range of uniform cluster lattices to the accuracy required for reactor stability studies. The void coefficient $k_v$ can be defined by

$$k_v = \frac{(dk/k)}{(d\rho/\rho)} = \frac{0{\cdot}72}{d\rho}\left(\frac{dk}{k}\right)$$

where $k$ can be written as $k$-infinity or $k$-effective, and $\rho$ is the coolant density which has an average value of 0·72 g/cm³ for the prototype under normal operating conditions. Stability studies had shown that the void coefficient for a large SGHW power reactor should ideally lie within the approximate range ±0·02 and the experiments were therefore designed to determine the void coefficients of the lattices tested to within ±0·01.

7. The results of this work were first discussed in references 3, 4 and 5 where it was shown that the experimental accuracies attained were, in general, adequate to meet the above criteria, although the use of discontinuous fuel limited the accuracy which could be achieved in material buckling measurements in the critical cores. Comparison of the experimental results with the predictions of the assessment code METHUSELAH I and the transport theory code THULE revealed some detailed discrepancies which are summarized in paras 25–33. Since that time, further development of METHUSELAH and the replacement of THULE by WIMS have improved the agreement between theory and experiment.

8. The later experiments were undertaken with a range of similar fuels containing varying proportions of plutonium and uranium oxides. The aims of the second series of measurements in regular cluster lattices were as follows:

(iv) to extend the comparisons required in (i)–(iii) above to include the range of fuel compositions resulting from operation of the SGHW prototype up to a mean fuel irradiation of 21 000 MWd/Te;

(v) to provide more detailed comparisons of predicted and measured void coefficients by using continuous fuel lengths to improve the accuracy of buckling determinations;

(vi) to test methods of predicting the effects of dissolving boron in the $D_2O$ bulk moderator.

### Experimental plant

The measurements described in this Paper were made in the following plant:

(i) DIMPLE—zero energy reactor with 8 ft 6 in. dia. tank for critical core studies;

(ii) JUNO—zero energy reactor, similar to DIMPLE but with 6 ft 3 in. dia. tank. JUNO was used to avoid reflector effects in critical core studies with limited quantities of $PuO_2/UO_2$ fuel;

(iii) SGHW I[17]—large exponential assembly using four antimony beryllium sources giving a thermal neutron flux of $5 \times 10^4$n/cm² sec for material buckling and power peaking measurements;

(iv) SGHW II[8]—sub-critical assembly with thermal neutron flux of $5 \times 10^7$n/cm² sec provided by the 10 kW NESTOR source reactor. SGHW II was used for the measurement of detailed reaction rates in the lattices which could not be taken critical.

### Range of lattices studied

The range of lattice geometries studied in the Winfrith experiments has been made sufficiently wide to provide a reliable test of the relevant methods of calculation. The clusters investigated ranged from 90 × 0·3 in. dia. fuel pins in a 5·25 in. i.d. pressure tube to 37 × 0·5 in. dia. pins in a 4·52 in. i.d. pressure tube. Only three lattice pitches were studied, since the pitch of the prototype was defined within fairly narrow limits at an early stage in the optimization studies, and calculations showed that at the chosen value, the neutron spectrum in a cluster is largely insensitive to variations in lattice pitch. The spectrum is, however, directly affected by the average coolant density in the cluster and a range of 'effective coolant densities' was therefore studied. These were selected from the following—the nomenclature used to denote the various coolants in this report are shown in parenthesis:

(i) light water (*WATER*);

(ii) light water/polystyrene bead mixture (*BEADS*) containing 0·04 g/cm³ of polystyrene with a slowing down power equal to that of light water of density 0·57 g/cm³;

(iii) light water/heavy water mixture (*MIXTURE*) containing up to 70% of $D_2O$ by weight and with a slowing down

power equal to that of light water in the density range 0·4–0·6 g/cm³;

(iv) air (*AIR*).

11. The leading parameters of the lattices investigated are summarized in Table 1, the corresponding values for the prototype being included for comparison. The arrangements of typical experimental lattice cells are shown in Figs 1 and 2.

Range of parameters measured

To meet the aims outlined in paras 6–8, the following measurements were made:

(i) material buckling[10] with additional measurements of critical moderator height and rate of change of reactivity with water height in the critical cores;

(ii) thermal fine structure[6] using U-235 and/or manganese foils;

(iii) Lu/Mn and Pu/U reaction rate ratios[9] normalized to thermal column values. (Thermal spectrum indicators);

(iv) the ratio of total capture in U-238 to fission in U-235 relative to the thermal column value of the same ratio.[7] (Relative conversion ratio, RCR);

(v) fission in U-238 relative to fission in U-235.[8] (Fast ratio, FR);

(vi) integral void coefficient inferred from the change in material buckling associated with a change in the coolant in each cell.

13. Each of the reaction rate measurements (ii)–(v) was made in a number of representative fuel pin positions so that

Table 1: *Uniform cluster SGHW lattices investigated during experimental physics programme*

| Lattice serial No. | *Pitch* S=square T=triangular (inches) | Fuel cluster[a] Material (% by wt.) U-235 | Pu-239 | Pu-240 | Pu-241 | Geometry[c] (inches) | Pressure[b] tube I.D. (inches) | Thickness (inches) | Volume ratio $V_{coolant}/V_{fuel}$ | $V_{moderator}/V_{fuel}$ | Coolants | Remarks |
|---|---|---|---|---|---|---|---|---|---|---|---|---|
| SG1 | 9·50T | 1·14 | — | — | — | 90×0·3 | 5·250 | 0·125 | 1·8 | 6·9 | A, W | |
| SG2 | 9·50T | 0·91 | — | — | — | 37×0·5 | 5·250 | 0·125 | 1·7 | 6·3 | A, W | |
| SG3[d] | 9·50T | 0·91 | — | — | — | 37×0·5 | 4·520 | 0·128 | 0·9 | 6·3 | A, M, B, W | 'Beads' coolant studied in SG3 only |
| SG5, SG6[d] | 9·50T | 0·91 | — | — | — | 37×0·5 | 4·520 | 0·128 | 0·9 | 6·3 | M, W | Reaction rate measurements in SGHW II only |
| SG4 | 9·50T | 0·91 | — | — | — | 37×0·5 | 4·520 | 0·128 | 0·9 | 7·3 | A, M, W | |
| SG11 | 9·50S | 1·78 | — | — | — | 90×0·3 | 5·250 | 0·125 | 1·8 | 8·8 | A, W | |
| SG12 | 9·50S | 0·91 | — | — | — | Outer 20×0·5 | 5·250 | 0·125 | 1·2 | 6·6 | M, W | |
| | | 1·78 | — | — | — | Inner 23×0·5 | | | | | | |
| SG13 | 9·50S | 1·35 | — | — | — | 71×0·4 | 5·250 | 0·125 | 1·2 | 6·3 | A, M, W | No moderator displacement tubes |
| SG13 | 9·50T | 1·35 | — | — | — | 71×0·4 | 5·250 | 0·125 | 1·2 | | M, W | Reaction rate measurements in SGHW II only |
| SG14 | 9·50S | 1·35 | — | — | — | 71×0·4 | 5·250 | 0·125 | 1·2 | 6·1 | A, M, W | Moderator displacement tubes empty |
| SG15(F) | 10·25S | 1·35 | — | — | — | 74×0·4 | 5·250 | 0·125 | 1·0 | 6·7 | M, W | Moderator displacement tubes flooded |
| SG15(E) | 10·25S | 1·35 | — | — | — | 74×0·4 | 5·250 | 0·125 | 1·0 | | M, W | Moderator displacement tubes empty |
| SG17($B_0$) | 10·25S | 1·35 | — | — | — | 74×0·4 | 5·250 | 0·125 | 1·0 | 6·7 | M | |
| SG17($B_1$) | 10·25S | 1·35 | — | — | — | 74×0·4 | 5·250 | 0·125 | 1·0 | 6·7 | M | Moderator poisoned with 2·20 ppm B10 |
| SG17($B_2$) | 10·25S | 1·35 | — | — | — | 74×0·4 | 5·250 | 0·125 | 1·0 | 6·7 | M | Moderator poisoned with 4·45 ppm B10 |
| SG19 | 10·25S | 1·35 | | | | 74×0·4 | 5·250 | 0·125 | 0·9 | 6·7 | M, W | |
| SGP1 | 10·25S | 0·906 | 0·230 | 0·015 | 0·001 | 74×0·4 | 5·250 | 0·125 | 0·9 | 6·7 | M, W | |
| SGP2 | 10·25S | 0·426 | 0·710 | 0·076 | 0·010 | 74×0·4 | 5·250 | 0·125 | 0·9 | 6·7 | M, W | |
| 100 MW(E) SGHWR prototype | 10·25S | 2·28 | — | — | — | 36×0·57 | 5·140 | 0·195 | 1·1 | 6·8 | 0·7–0·2 g/cm³ | Moderator displacement tubes flooded |
| | | 1·56 | — | — | — | | | | | | | |
| | | 1·24 | — | — | — | 36×0·57 | 5·140 | 0·195 | 1·1 | 6·3 | 0·7–0·2 g/cm³ | Moderator displacement tubes empty |

*Notes:* (a) The fuel for lattices SG1 to SG12 was in welded aluminium cans, 0·036 in. thick in 14 in. or 28 in. lengths. Subsequent fuel was canned in 0·020 in. aluminium, but apart from the SG13 and SG14 cores, it was in continuous lengths.
(b) Aluminium was used in the experiment in place of Zircaloy.
(c) Up to SG14 the centre of each cluster was occupied by a standard fuel pencil except in cores SG1 and SG11 where steel tie bars 0·5 in. dia. were used. Cores SG1 *et seq.* contained air filled standard aluminium fuel cans in the central positions.
(d) Lattices SG3, 5 and 6 represent three different methods of reducing $V_{moderator}/V_{coolant}$ relative to lattice SG4 by displacing $D_2O$ with air. This makes the void coefficient more negative.

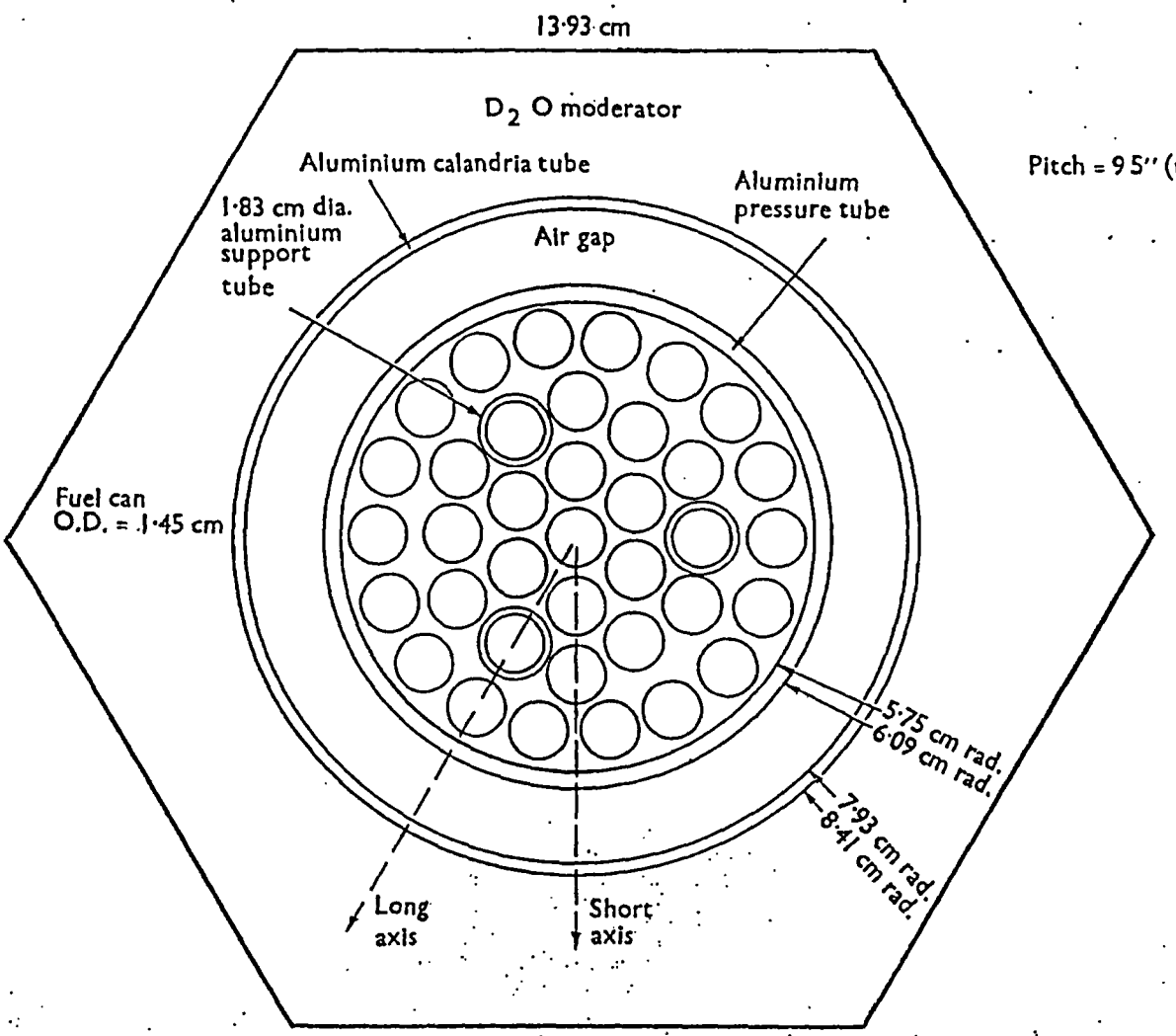


*Fig 1* Lattice cell for core SG3

cluster distributions as well as average cluster values are available for comparison with theoretical predictions. In view of the sensitivity of reactivity and void coefficient to the RCR value in these lattices (1% in RCR≈0·3% in $k$-infinity), particular emphasis has been placed on the accurate determination of this parameter and measurements of U-238 capture have been made by both coincidence[7] and chemistry[18] techniques in each case.

14. From the measured material bucklings a value of $k$-infinity (Leakage) can be obtained. This, however, requires theoretical leakage parameters which, in these cases, have been obtained by a Benoist technique.[19] It is desirable to have an alternative method of determining $k$-infinity which does not involve leakage parameters and this is feasible in cases where there is a complete set of detailed reaction rates available. The differences between the theoretical and experimental reaction rates are used to correct the theoretical $k$-infinity to give $k$-infinity (Reaction Rate) as described in detail in reference 20. Complete sets of reaction rate measurements were made in cores covering a wide range of SGHW lattices, and it is shown in para. 96 (see Tables 14 and 15) that for liquid cooled cores the average discrepancy between $k$-inf (Leakage) and $k$-inf (Reaction Rate) is $+0{\cdot}18 \pm 0{\cdot}60\%$, thus giving some confidence that no significant systematic errors are present in the measurements.

### Development of experimental techniques

The experimental techniques used to measure detailed reaction rates in SGHW lattices were described in a number of reports[6–10] during 1964. Since that time, some developments have taken place and further calibrations have been undertaken, so that slightly modified values of improved accuracy are now available for comparisons with theory.

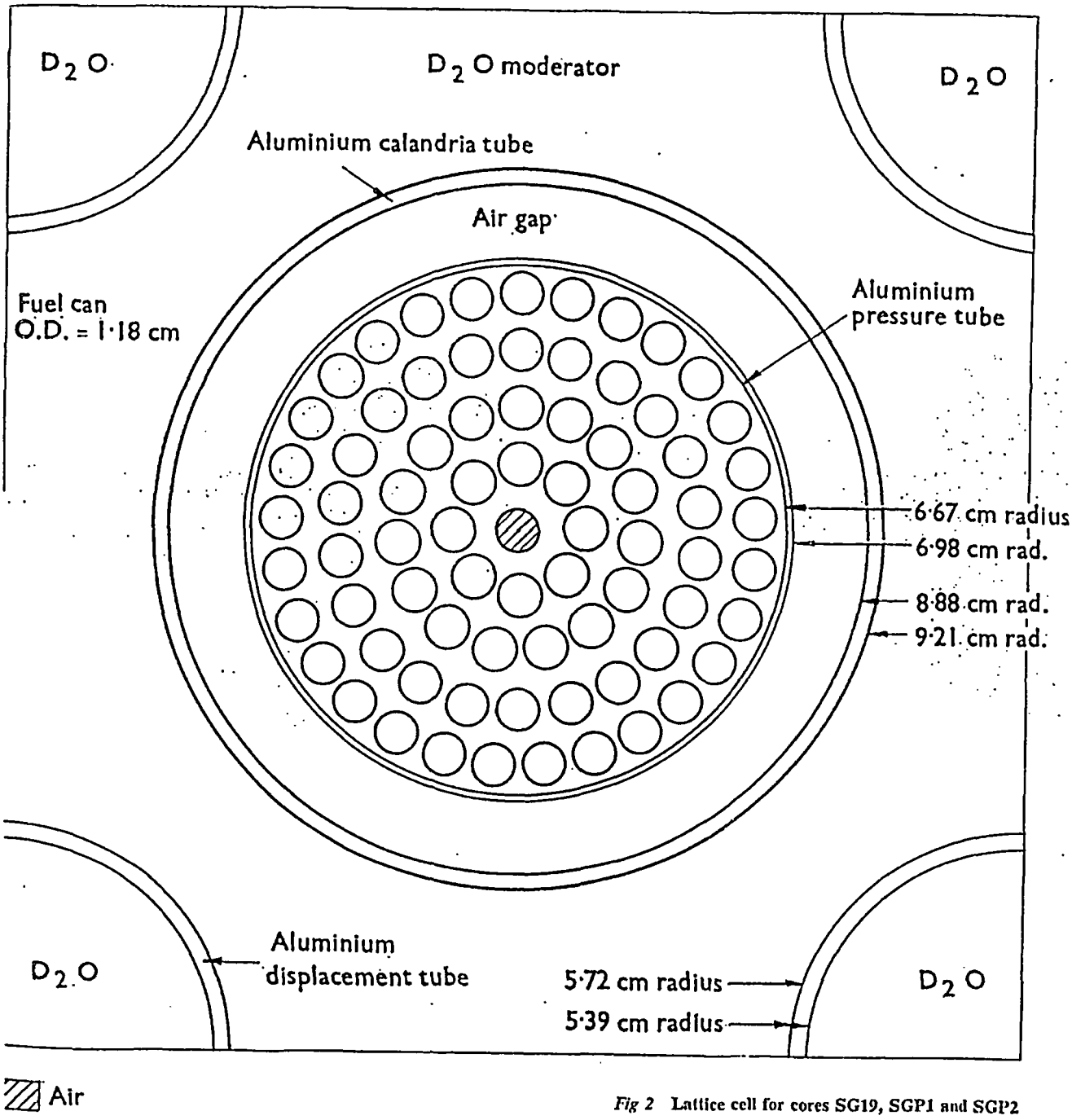


*Fig 2* Lattice cell for cores SG19, SGP1 and SGP2

The important changes are described in the following paragraphs.

*Calibration of U-238 fast fission measurements*

Fast fission in U-238 is determined by the 'double-enrichment' method which yields a value of the U-238/U-235 fission-activity ratio $(F_8/F_5)_\gamma$, varying with the time of counting the foils after an irradiation of specified duration. This ratio must be related to the true fast fission ratio $(F_8/F_5)$ and a time dependent calibration factor $P(t)$ is therefore defined as

$$P(t) = \frac{(F_8/F_5)}{(F_8/F_5)_\gamma}.$$

17. $P(t)$ was measured in a cadmium covered double fission chamber positioned close to one face of the source reactor NESTOR so that an adequate U-238 fission rate could be obtained. The flux in the chamber was markedly anisotropic and subsequent measurements have shown that linear interpolation of the neutron spectrum conditions from the positions of the thin uranium deposits used to measure the fission rates, to the intervening positions of the foils for subsequent $\gamma$-counting, was introducing a systematic error. $P(t)$ has now been redetermined by two more satisfactory methods. The double fission chamber experiment has been redesigned so that the uranium deposits and the foils are only 0·006 in. apart, thus minimizing the error which can be introduced by lack of a detailed knowledge of the spatial variation of the spectrum in the chamber. In the second method, use was made of absolute parallel plate type U-235 and U-238 fission chambers which have been developed by Broomfield and Stevenson[21] for use in fast reactor studies in ZEBRA[22] at Winfrith. International intercalibration of chambers of this type has shown[21] that the sensitivities of these chambers are known to about ±1%. A comparison of the sub-cadmium counting rates of two such chambers of widely differing enrichment, placed successively in a fixed position near a face of NESTOR, can thus be used to define the true fission rate in a foil inside a dummy fission chamber placed at the same position. Gamma counting of the foil then yields $P(t)$ as before.

18. The results from the two types of measurements were as follows, 240 minutes after a two hour irradiation.

Double fission chamber: $P(240\text{ min}) = 1{\cdot}33 \pm 0{\cdot}03$
ZEBRA fission chamber: $P(240\text{ min}) = 1{\cdot}32 \pm 0{\cdot}04$

These values are somewhat higher than the previous calibration factor which was quoted in reference 4 as 1·22±3% (random) ±5% (systematic) and the following mean value has now been adopted:

$$P(240\text{ min}) = 1{\cdot}33 \pm 0{\cdot}03.$$

19. In addition to the absolute value of $P(240\text{ min})$, the above new measurements have provided more accurate information on the time dependence of $P(t)$. Analysing a range of lattices with the original and revised time dependence in the data reduction programme, it has been shown that for both 2 hour and 4 hour irradiation periods,

$$\frac{\text{FR (new time dependence)}}{\text{FR (original time dependence)}} = 0{\cdot}975 \pm 0{\cdot}005.$$

The values originally quoted for lattices SG1–SG13 in reference 4 have therefore been increased by

$$\frac{1{\cdot}330}{1{\cdot}217} \times 0{\cdot}975 = 1{\cdot}068.$$

The 0·5% uncertainty in the change in the effect of time dependence has been taken into account in assessing the systematic errors of the FR measurements. In addition, since the great majority of the latest measurements of $P(t)$ have used 2 hour irradiation times, results from the early fission ratio measurements SG1–SG6 which used 4 hour irradiation periods may be subject to slightly larger errors and an additional ±1% contribution to the total systematic uncertainty has therefore been allowed in these cases.

*Fission product breakthrough in coincidence measurement of U-238 capture*

The determination of U-238 capture by the coincidence counting of Pu-239 $\gamma$ and X-rays is perturbed by unwanted coincidences from the fission product background. A correction factor $Q(t)$ must therefore be determined such that

$$Q(t) = \frac{\text{Observed fission product coincidence count rate per U-238 atom}}{\text{neptunium-239 coincidence count per U-238 atom in the absence of self-absorption}}$$

21. $Q(t)$ is determined in a separate experiment in which $UO_2$ foils of widely differing enrichment are irradiated in a thermal flux for the standard period and then coincidence counted alternately. Recent check measurements using a range of foil enrichments have shown that $Q(t)$ is markedly sensitive to details of the foil and counter geometries and can be significantly different (e.g. 25%) for upper and lower counters which are nominally identical. New measurements of $Q(t)$ have been made for each counter using foils which are identical to those used for RCR measurements in everything except enrichment, and it has been shown that on average the common value of $Q(t)$ assumed in reference 4 should be increased by about 26%. The correction to RCR from fission product breakthrough may be approximated by

$$\left[1 + \frac{Q(t)}{a} \cdot \frac{N_5}{N_8}\left(1 - \frac{1}{\text{RCR}}\right)\right]$$

where $a$ is the $\gamma$-ray transmission factor of the foil ($\approx 0{\cdot}6$) and $N_5/N_8$ is the number ratio of atoms. In the present cores, RCR$\approx$2 and for a typical enrichment of 1·35% the correction to RCR is about +1·7%. A change in $Q(t)$ of +26% thus increases the fission product correction to 2·1%, a rise of 0·4% in RCR. Appropriate corrections of similar magnitude have been applied to all the RCR values from reference 4 as shown in Table 6 of para. 57.

*Increased escape probability of $\gamma$ and X-rays from edge of $UO_2$ foil during coincidence counting*

During the coincidence counting of Pu-239 activities, $\gamma$ and X-rays emitted near the periphery of the $UO_2$ foil are less likely to be absorbed by the foil material. This decreased self-absorption affects both the thermal column and the lattice foils, but it is more important in the latter case since the radial distribution of U-238 capture in the lattice foil is strongly biased towards the periphery. In the comparisons between theory and experiment in reference 4, a correction of −0·4% was applied to RCR to compensate for this effect, based on the calculation by Leslie described in Appendix 1 of reference 7. Recent experimental work by Taylor *et al.*[23, 24] using $UO_2$ guard rings accurately matched to the foils has implied a smaller correction of about −0·2%. A correction of this magnitude has therefore been applied (see Table 6), allowing as before a possible additional contribution of ±0·2% as a random systematic uncertainty.

*Residual discrepancy between coincidence and chemistry determinations of U-238 capture*

As a check on the absence of significant systematic error in the coincidence counting of Pu-239 activities, the RCR is

Table 2: *Comparison of coincidence and chemistry determinations of RCR*

| Fuel enrichment | Coolant | RCR: Coincidence | RCR: Chemistry | Discrepancy of chemistry results from coincidence in % |
|---|---|---|---|---|
| 1·24% | 50% $D_2O$/ 50% $H_2O$ | 1·876 | 1·882 | +0·32% |
| 1·56% | 50% $D_2O$/ 50% $H_2O$ | 1·989 | 1·992 | +0·15% |
| 2·28% | 50% $D_2O$/ 50% $H_2O$ | 2·352 | 2·364 | +0·51% |
| 0·8% $PuO_2/UO_2$ | 51% $D_2O$/ 49% $H_2O$ | 2·512 | 2·522 | +0·40% |

remeasured in about 20% of the fuel pin positions using a chemical separation technique[18] followed by singles counting of the plutonium $\gamma$-activity above 53 keV. An early comparison of corresponding results from the two techniques in reference 4 yielded random discrepancies averaging about 2%. Later, more accurate measurements revealed the existence of a trend varying with enrichment. For a typical SGHW enrichment of 1·35%, the RCR determined by chemical separation was about 2% higher than the coincidence value, while for 3% $UO_2$ the discrepancy was 4%. Three main improvements in the technique have now been introduced:

(a) fission product breakthrough factors $Q(t)$ have been determined accurately for each scintillation counter as described in para. 21 above;

(b) comparative RCR measurements have been made with the co-operation of AB Atomenergi. Fuel packs were irradiated in pairs at Winfrith, the foils from the two packs being counted at Studsvik, Sweden and at Winfrith respectively. These comparisons have shown the importance of avoiding perturbations leading to thermal and/or resonance flux variations along the fuel packs, particularly in cases where the foils used for coincidence counting are positioned a finite distance from the pellet used for the chemical separation. The fuel packs used for RCR measurements at Winfrith have been increased in length from 3 cm to 5 cm to move the small inter-pack air gaps ($\approx$0·03 in.) further away from the positions of measurement. In addition, the depleted metal guard foils on either side of the depleted foil have been reduced in thickness from 0·003 in. to 0·001 in. These changes have reduced the average discrepancy between coincidence and chemistry results by about 0·3%;

(c) in some cases the $UO_2$ powder supplied for making up the accurately dimensioned foils and pellets for RCR determinations had been obtained from reprocessed material and contained significant impurities (e.g. plutonium) which complicated the chemistry determinations. Fresh $UO_2$ of high purity is now specified and check measurements by a spectroscopy are made before the pack components are fabricated. Recent careful comparisons of the techniques which are believed to be free from the above sources of systematic error gave the results shown in Table 2.

These results indicate a small discrepancy between the two techniques, which appears to increase with enrichment, the chemistry determinations being the higher. Other recent measurements have included checks of this discrepancy with enrichments up to 3% and have shown average discrepancies for each fuel studied of up to 1%, confirming that any bias is small. Since the previous discrepancies were 2% and 4% respectively, this represents a marked improvement, but it should be noted that the known changes incorporated in the technique are not sufficient to explain the difference. Until a satisfactory explanation can be found, one cannot be completely certain that no unknown systematic error is present.

*Improved accuracy in the determination of the coolant void coefficient*

In the cores studied in the first stage of the SGHW programme, (SG1–SG14), the use of discrete fuel lengths and the presence of significant cluster end plates in the core limited the accuracy of the void coefficient ($k_v$) inferred from the change in material buckling with effective coolant density. The main test of the theoretical methods of predicting void coefficient was by comparison with values of $k$-inf (Reaction Rate), and it was shown[6] that the void coefficient (as defined in para. 6) could be determined in this way to within an absolute uncertainty of $\pm$0·01. The use of continuous fuel lengths in the subsequent cores SG15 *et seq.* has resulted in a great improvement in the accuracy of the bucklings measured in these cores. Since the integral void coefficient of $k$-inf for regular cluster lattices can be inferred from buckling measurements at two extreme effective coolant densities (see para. 6), this produced a corresponding improvement in the accuracy of determinations of the void coefficient, e.g. between effective densities of 1·0 g/cm$^3$ and 0·4 g/cm$^3$ the void coefficient can be determined to an absolute accuracy of $\pm$0·005.

## THEORETICAL METHODS

### Defects in previous methods

The experimental results from the early regular cluster lattices SG1 to SG13 were compared in references 3 and 4 with theoretical predictions using the codes METHUSELAH I[11] and THULE.[12] Although the agreement between theory and experiment was, in general, satisfactory, there were a number of discrepancies in detail which pointed to the need for further development of the calculational methods. These discrepancies are summarized below, attention being concentrated on the liquid cooled experimental lattices (see para. 10) which are more relevant to the performance of the prototype.

*Fast fission U-238*

METHUSELAH I overestimated U-238 fission by 10–15%, but the renormalization of the fission ratio measurements described in section 19 implies that the overestimate will now be reduced to 5–10%. The variation with coolant density is correctly predicted. The use of diffusion theory coupled with the neglect of fast hyperfine structure and the particular choice of U-238 cross-sections thus introduce errors which cancel as far as their contribution to void coefficient is concerned. The THULE calculation underestimates U-238 fission with water coolant and overestimates the variation with coolant density. The calculation does not include hyperfine structure in the fast energy group,

and if this had been included, the prediction of U-238 fission would be improved. An approximate correction applied in four typical liquid cooled cores yielded calculated values of fission ratio averaging 9% below the renormalized experimental values.

*Resonance capture*

METHUSELAH I underestimates the relative conversion ratio by 1·7% on average, which implies an underestimate of U-238 resonance capture by about 3% if all of the discrepancy is attributed to this cause. The THULE calculation of resonance events used the MOCUP Monte Carlo code[25] with 8–10 000 source neutrons for each case, starting with a flat flux assumption at 10 keV. In spite of the statistical variations introduced by the Monte Carlo method, there was definite evidence from the water and mixture cooled lattices that THULE overestimates the relative conversion ratio, and it was shown that theory and experiment could be brought into much better agreement if the absorption resonance integral of U-238 were reduced by about 7½%. Results from lattices SG3 and SG13 of Table 1 gave somewhat anomalous values; SG3 was taken as a test case and the Monte Carlo calculations repeated using 100 000 neutrons with results in good agreement with the general trend.

*Thermal fine and hyperfine structure*

Provided that the scattering cross-sections used in the calculation are consistent with the measured values of the thermal diffusion coefficients in $H_2O$ and $D_2O$, the calculated fine structure in SGHW systems is largely insensitive to the particular thermalization model used. In the clusters containing large numbers of pins (≈70), the ring smearing model used in both METHUSELAH I and THULE should be valid. In such cores, METHUSELAH I underestimates the fine structure for mixture coolant but overestimates it for water coolant and hence over-emphasizes the importance of fine structure changes on the void coefficient. In the clusters containing smaller numbers of pins of larger diameter, both METHUSELAH I and THULE consistently underestimate the fine structure, but the METHUSELAH I prediction of the variation with coolant density is better than the THULE prediction.

29. Thermal hyperfine structure in individual pin cells was calculated by the RIPPLE[26] slab collision theory programme in both METHUSELAH I and THULE, assuming one thermal neutron group only. Comparison with sector foil manganese reaction rate measurements in fuel and coolant positions showed that RIPPLE consistently underestimated thermal hyperfine structure by about 3%.

*Thermal neutron spectrum*

Comparison of measured and predicted values of the plutonium/uranium fission and lutecium/manganese reaction rate ratios show that METHUSELAH I predicts too soft a neutron spectrum as might be anticipated from its use of a gas model for $H_2O$. The width model used in THULE[12] leads to a harder calculated spectrum but still underestimates the lutecium/manganese ratio by about 3½% on average in the liquid cooled cores. Changing from a gas model to an effective width model for the $D_2O$ moderator hardens the cluster spectrum significantly, particularly in the outer rings, and hence improves the agreement between predicted and measured average cluster spectra. However, THULE predicts too soft a spectrum in the centres of liquid cooled clusters relative to the outer rings, thus over-emphasizing the penetration into the cluster of the thermal neutrons formed in the $D_2O$.

*Reactivity*

METHUSELAH I overestimates $k$-infinity of liquid cooled cores by about 1½% in reactivity, mainly due to overestimating U-238 fission and underestimating U-238 capture. The overlapping thermal group model in METHUSELAH I breaks down in air-cooled cores where the source of fuel spectrum neutrons goes to zero. This leads to an average $k$-infinity overestimate of 4% for these cores. The METHUSELAH I eigenvalues are closer to unity than these discrepancies in $k$-infinity suggest, since a tendency to overestimate leakage provides a compensating effect.

32. THULE predicts $k$-infinity for both liquid and air-cooled lattices to within ±1% and reactivity to ±1½% or better.

*Void coefficient*

An investigation of the random and systematic errors present in the experimental measurements has shown[5] that the void coefficient as defined in para. 6 has been determined to an accuracy of ±0·01. Both methods of calculation have been shown to predict the void coefficient within these limits.

**The improved assessment and design code METHUSELAH II**

METHUSELAH is a FORTRAN language programme which calculates reactivity and reaction rates for a cell in an infinite array of such cells in a liquid moderated reactor. A five-group diffusion theory technique is used. The three fast groups cover the energy ranges 10 MeV to 0·821 MeV, 0·821 MeV to 5·53 keV, and 5·53 keV to 0·625 eV. Two overlapping thermal groups are used, one of which (group 4) is generated in the fuel cluster region and removed in the bulk moderator, the other (group 5) is generated in the bulk moderator and removed in the fuel cluster region. The effective cross-sections for these two groups are obtained from a Wigner–Wilkins spectrum compilation, the removal cross-sections being obtained by the method described by Leslie in reference 27. In the METHUSELAH I version[11] spectra were typified by an infinite fuel cluster and an infinite bulk moderator with spectrum hardening corrections for net leakage into or out of these regions. The version used in this report is METHUSELAH II.[13]

35. In METHUSELAH II the nuclear library has been revised. In particular, an allowance is now made for the effect of absorption on the transfer cross-section between the overlapping thermal groups. At low coolant densities there is very little moderation within the fuel cluster and therefore in the METHUSELAH I calculation very little source to drive group 4. Thus most of the neutrons within the cluster belong to the group 5 soft spectrum. This is physically absurd as the spectrum in an air-filled cluster should clearly be harder than in a water cooled cluster. In METHUSELAH II, group 5 neutrons are successively

transferred to group 4 as the neutrons diffuse into the cluster. This transference is derived entirely from the absorption cross-sections and is additional to the transfer cross-section resulting from moderating collisions. The details of the changes made in METHUSELAH II are described in reference 13.

36. Because of the large mean free paths in the highest energy group, the use of diffusion theory in METHUSELAH leads to an underestimate of the group 1 flux in the fuel cluster. Normalization of the METHUSELAH predictions to a more exact calculation is therefore required. A set of new group 1 U-238 cross-sections weighted by a fuel flux enhancement factor has therefore been derived from SPEC[28] Monte Carlo calculations for the typical SGHW lattices of the prototype core, and these are now included in METHUSELAH II.

37. The parameters for the group 3 U-238 resonance absorption cross-section have been revised and incorporated into METHUSELAH II. These parameters are based on Hellstrand's single rod measurements of resonance integral[29] whereas in METHUSELAH I they were based on Hellstrand's cluster measurements.[30]

38. The normalizing factors, which scale the Wigner–Wilkins cross-section tabulations for each isotopic reaction, have been revised in METHUSELAH II. Thus the magnitudes of the cross-sections are changed but not the spectrum variation. Many of the lattices in Table 1 have aluminium moderator displacement tubes at the interstitial positions, which do not fit easily into the cylindrical cell representation adopted in METHUSELAH. In order to incorporate these tubes, therefore, they are transformed into thin annuli of the same volume around the bulk moderator; the displacement tube contents (air or $D_2O$) then form the outermost annulus of the cell. The process is shown in Fig. 3; it will be seen that the displacement tube is turned inside out. One result of the approximation is that the displacement tube and content annuli are thin; thus METHUSELAH shows very little flux variation across the annuli, a result not necessarily true for the real displacement tube.

39. Improvements in the efficiency of the programme have been made. There are also additional facilities such as burn-up and fuel cost routines which, however, do not affect the experimental analysis. Neutron leakage typically accounts for 15% of all events in a critical experimental core in DIMPLE, whereas the corresponding figure for the prototype is about 3%. To cater for the increased importance of these events in the experimental cores, a modified version of METHUSELAH II (known as NOAH II[31]) is available incorporating BENOIST[19] leakage calculations. In cases where the moderator displacement tubes are empty, a further streaming correction is applied by hand, using the method reported in Appendix 2 of reference 4. For the remainder of this Paper, in which experimental results are compared with theory, METHUSELAH values are obtained from the METHUSELAH II version of the code.

### The Winfrith Improved Multi-group Scheme, WIMS

The more sophisticated method is the WIMS code[14] which is an outgrowth of TRACER[32] and THULE.[12] WIMS has been designed to perform detailed lattice cell calculations for a variety of moderators and geometries, and provides

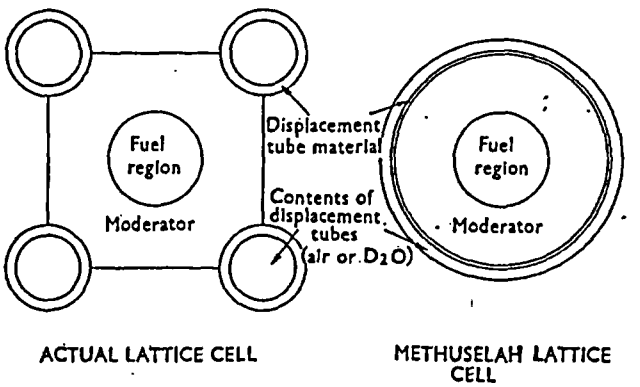


*Fig 3* Representation of displacement tubes used in METHUSELAH and WIMS

the opportunity to compare results for different types of reactor (including both thermal and fast reactors) using similar models and common data sets. Both elaborate calculations in many groups and more rapid computations in few groups for assessment purposes are possible using consistent methods and data.

41. The physics methods adopted in WIMS have been described by Askew *et al.*[33] and a detailed study of WIMS calculations on regular light water lattices has been given by Fayers *et al.*[34] A further study of WIMS calculations on heavy water moderated clusters (embracing SGHW lattices and the Canadian ZED lattices) is shortly to be published[16] and a selection of the results from this study are included in the present Paper. A selection of WIMS calculations on both single rod and cluster geometries with graphite and water moderation were also included in a paper[35] delivered at the recent BNES conference on 'Physics Problems in Thermal Reactor Design'. This latter paper also describes some of the theoretical checks which have been made of the WIMS methods by comparison with more sophisticated (e.g. Monte Carlo) codes.

42. For convenience we include a résumé of the WIMS methods in this Paper. The basic cross-sectional library is in 69 groups with 14 of these groups spanning the high energy region from 10 MeV to 9·118 keV, 13 groups in the resonance region above 4 eV, and 42 thermal groups. With certain exceptions given below, the group constants are formed from the Winfrith Nuclear Data File[36] using suitable weighting spectrum in the GALAXY code.[37] One exception to this rule is the thermal scattering data which include the Nelkin and Haywood models for $H_2O$, the Honeck model for $D_2O$ and the Egelstaff model for graphite. The WIMS calculations presented in this Paper have used the Nelkin and Honeck models for light and heavy water respectively, and a gas model for all other elements.

43. The resonance treatment uses equivalence theorems to relate a group resonance integral for the heterogeneous cell to group resonance integrals for homogeneous mixtures. The library of resonance integrals has been compiled using the SDR code[38] which provides a numerical solution of the slowing down equations in the presence of a resonance absorber using some 120 000 energy points. Special procedures are used in the WIMS resonance treatment to

estimate the depression in flux which is needed to form absorption and fission yield cross-sections, and to adjust the group removal cross-sections. The provision of a number of groups in the resonance region allows a varying source shape to have its proper influence on resonance captures. This effect can be particularly important in cluster geometries. This deterministic resonance treatment, which is shown to compare favourably with Monte Carlo calculations in reference 35, represents a large saving in computer time in comparison with THULE, e.g. for a typical 36-pin cluster, a WIMS cell calculation on the KDF9 computer takes about 20 minutes which is at least a factor of three quicker than the corresponding THULE calculation.

44. A preliminary flux solution using the full number of library groups but a simplified spatial treatment, known as the SPECTROX method[39] is used to generate a small number of condensation spectra. In cluster geometry these apply to fuel, clad, coolant and moderator. A detailed geometric solution of the transport equation using condensed cross-sections follows, using either the DSN or collision probability methods. The PIJ collision probability option,[40] in particular, allows a detailed representation of cluster geometries and obviates the need for ring smearing. The results quoted in the present Paper, unless stated otherwise, are derived by the DSN method.

45. Various methods are included for performing leakage calculations which include both the diffusion theory and $B_1$ methods with BENOIST prescriptions[19] for diffusion asymmetry. The WIMS results quoted in this Paper all involved the three-region BENOIST streaming model option applied to a $B_1$ leakage calculation.

## SURVEY OF REACTION RATE COMPARISONS

### Introduction

The results of the measurements of detailed reaction rates in the lattices of Table 1 are compared with theoretical predictions in this section. In the early lattices studied, the fuel was in the form of discrete sections, 14 in. or 28 in. long, separated by fairly substantial end fittings. The reaction rate measurements were made at positions well away from these end fittings where it was confirmed experimentally that the values obtained were insensitive to axial positioning.

47. In measuring the relative conversion ratio, considerable care is taken to minimize the perturbation of the lattice at the measuring position by using accurately matched $UO_2$ discs of the same enrichment as the adjoining fuel pellets. In other cases, however, some perturbation is inevitable, e.g. when measuring hyperfine structure or the lutecium/manganese reaction rate ratio; in such instances suitable correction factors have been applied as described in reference 5, so that the quoted experimental results refer to infinitely dilute values of the reaction rates concerned within the stated limits of random and systematic error. All such corrections applied to the raw experimental data are listed in the tables or defined in the text.

48. In cases where the cluster average values of a reaction rate ratio is required, this has been obtained by summing the individual reaction rates weighted by the appropriate number of fuel pins in each ring, and then dividing the two cluster average values so obtained. To conserve space, only these average values are compared with the corresponding theoretical predictions, but complete cluster distributions are quoted in references 15 and 16 and a few typical examples are illustrated in this Paper. The experimental uncertainties shown in the figures are statistical counting errors only. Systematic errors are quoted in the relevant tables.

### Fast fission in U-238

*Cluster average values*

Values of the U-238/U-235 fission ratio averaged over the fuel cluster are compared with theory in Table 4. The fission ratio and relative conversion ratio are measured in modified fuel packs in demountable fuel pins which have marginally different diameters and oxide densities from the standard fuel. The PIJ[40] collision theory option of WIMS has been used to investigate the effects of such differences in the central pin of a simplified square array of 0·4 in. diameter, 3% enriched $UO_2$ pins in an $H_2O$ moderator. To highlight these effects, rather extreme variations of 10% in the numbers of U-238 atoms have been considered. After the SPECTROX solution the main PIJ solution was performed in four neutron energy groups and the results are given in Table 3. Comparative calculations have been carried out for equivalent situations using the cluster option in METHUSELAH, although in this case it is not possible to treat the problem in the same detail. In particular, the calculation of the Dancoff factor in the METHUSELAH calculation assumes that the central pin is surrounded by similar pins.

50. The results show that a 10% decrease in the number of U-238 atoms in the central pin resulting from a reduction in either diameter or density has a fairly small effect on the local fast flux but will lead to increased resonance absorption due to the reduced self-shielding in the pins. When measuring fission ratio or relative conversion ratio, there is the additional effect of an increase in local thermal flux caused by the removal of thermal absorber, giving net effects on FR and RCR of $-2{\cdot}2\%$ and $+0{\cdot}8\%$ in the worse cases. METHUSELAH calculations for the same cores give net effects of $-1{\cdot}7\%$ and $+1{\cdot}2\%$ which are not greatly in conflict with the WIMS conclusions. (The predictions of fast flux may suffer from numerical errors of up to 0·5%.) Typically, the fuel in the demountable pins is 0·010 in. smaller in diameter and 0·2 g/cm³ greater in density than a standard pin, and approximate corrections to FR of $+0{\cdot}1\%$ and $-0{\cdot}4\%$ respectively are required, with smaller corrections for RCR. These corrections are small compared with the appropriate systematic experimental errors and they have therefore been neglected in presenting the experimental results in Tables 4 and 6.

51. The figures in Table 4 show that in the liquid cooled clusters, the significant overestimate of fast fission events by METHUSELAH I has been virtually eliminated by the renormalization of the U-238 fast cross-sections to the results of SPEC[28] Monte Carlo calculations for the SGHW prototype. Since the normalization runs used an average prototype coolant density, it is not surprising that the agreement between METHUSELAH II and experiment is poorer for air-filled clusters, but even in these cases the average discrepancy of $4{\cdot}2\%$ is worth only about $0{\cdot}1\%$ in reactivity.

52. The WIMS predictions are consistently low although the variation with coolant density is reasonably accurate.

In view of the multi-group transport methods used to calculate fast effects in WIMS, this performance is disappointing. However, it was shown in para. 26 that renormalization of the SGHW fast fission measurements leads to an average underestimate of 9% by the THULE code[12] and similar discrepancies with the predictions of sophisticated codes have been reported elsewhere.[35]

53. Checks on the WIMS method using the Monte Carlo code SPECIFIC[41] have been hampered by mechanical difficulties in inserting identical data into the two codes. Further information on these tests will be reported later,[16] but preliminary indications are that the WIMS methods underestimate U-238 fission slightly but are unlikely to produce an underestimate of more than about 5% in U-238 fissions. SPECIFIC differs from the SPEC Monte Carlo code[28] used to normalize the METHUSELAH fast group cross-sections, in that SPECIFIC treats individual fuel pins whereas ring smearing is used to describe cluster geometry in the SPEC code. However, in multi-pin clusters of the SGHW type, the effect of this difference should be small and it is therefore clear that some significant differences in nuclear data exist between the WIMS–SPECIFIC comparisons and the SPEC calculations which lead to such good agreement between METHUSELAH and experiment. The fast cross-sections used in WIMS are derived from carefully evaluated data in the UKAEA Nuclear Data Library.[36] A trial calculation has shown that if the inelastic scattering cross-section were decreased and the U-238 fission cross-section increased by amounts just compatible with a current alternative nuclear data set, the fission ratio would increase by only about 5%. Combining this with the underestimate of up to 5% shown possible by the WIMS–SPECIFIC comparison leads to a maximum underestimate of 10% compared with an average discrepancy with experiment of $10{\cdot}6 \pm 3{\cdot}2\%$. The possibility of some unsuspected systematic error in the experimental determination of fission ratio cannot therefore be ruled out and further measurements by an alternative technique are planned to provide further evidence on this point.

Table 3: *Effects of diameter and density differences on FR and RCR*

| Type of central pin | Reaction rates in central pin | | | | | | | | | |
|---|---|---|---|---|---|---|---|---|---|---|
| | U-238 fissions/atom | | U-238 captures/atom | | U-235 fissions/atom | | RCR | | FR | |
| | WIMS | METHUSELAH | WIMS | METHUSELAH | WIMS | METHUSELAH | WIMS | METHUSELAH | WIMS | METHUSELAH |
| Standard | 0·0467 | 0·0459 | 0·344 | 0·346 | 17·62 | 17·58 | 4·06 | 4·13 | 0·0846 | 0·0832 |
| 10% Reduced density | 0·0466 | 0·0457 | 0·354 | 0·356 | 17·97 | 17·84 | 4·09 | 4·18 | 0·0827 | 0·0818 |
| 5% Reduced diameter | 0·0472 | 0·0457 | 0·347 | 0·353 | 17·73 | 17·77 | 4·07 | 4·16 | 0·0849 | 0·0821 |

Table 4: *Cluster average values of U-238/U-235 fission ratio*

| Core | Coolant | Fission ratio | | | | | | |
|---|---|---|---|---|---|---|---|---|
| | | Expt. | Random error % | Systematic error % | METHUSELAH II | Discrepancy % | WIMS | Discrepancy % |
| SG1 | Air | 0·0516 | ±2·9 | ±4·2 | 0·0524 | +1·6 | 0·0490 | − 5·0 |
| SG1 | Water | 0·0381 | ±3·9 | ±4·2 | 0·0382 | +0·3 | 0·0340 | −10·8 |
| SG2 | Air | 0·0639 | ±2·3 | ±4·2 | 0·0592 | −7·4 | | |
| SG3 | Air | 0·0676 | ±2·1 | ±4·2 | 0·0642 | −5·0 | 0·0597 | −11·7 |
| SG3 | Mixture | 0·0547 | ±2·1 | ±4·2 | 0·0554 | +1·3 | 0·0493 | − 9·9 |
| SG3 | Beads | 0·0600 | ±2·2 | ±4·2 | 0·0581 | −3·2 | | |
| SG3 | Water | 0·0531 | ±2·1 | ±4·2 | 0·0535 | +0·8 | 0·0484 | − 8·9 |
| SG3 | Warm Water | 0·0533 | ±4·2 | ±4·2 | 0·0539 | +1·1 | | |
| SG4 | Mixture | 0·0528 | ±2·1 | ±4·2 | 0·0533 | +0·9 | 0·0479 | − 9·3 |
| SG4 | Water | 0·0516 | ±2·2 | ±4·2 | 0·0516 | 0·0 | 0·0470 | − 8·9 |
| SG5 | Mixture | 0·0537 | ±2·2 | ±4·2 | 0·0553 | +3·0 | | |
| SG5 | Water | 0·0505 | ±2·2 | ±4·2 | 0·0535 | +5·9 | | |
| SG6 | Mixture | 0·0570 | ±2·2 | ±4·2 | 0·0553 | −3·0 | | |
| SG6 | Water | 0·0530 | ±2·1 | ±4·2 | 0·0535 | +0·9 | | |
| SG12 | Mixture | 0·0525 | ±1·3 | ±3·2 | 0·0533 | +1·5 | 0·0481 | − 9·4 |
| SG12 | Water | 0·0518 | ±1·3 | ±3·2 | 0·0507 | −2·1 | 0·0470 | − 9·3 |
| SG13 | Air | 0·0700 | ±1·1 | ±3·2 | 0·0656 | −6·3 | 0·0600 | −14·3 |
| SG13 | Mixture | 0·0524 | ±1·3 | ±3·2 | 0·0528 | +0·8 | 0·0456 | −13·0 |
| SG13 | Water | 0·0521 | ±1·3 | ±3·2 | 0·0503 | −3·5 | 0·0449 | −13·8 |
| SG19 | Water | 0·0538 | ±1·0 | ±3·2 | 0·0524 | −2·6 | 0·0465 | −13·6 |
| | | | | *Average discrepancies:* | Air | −4·3 | | −10·3 |
| | | | | | Mixture | +0·8 | | −10·4 |
| | | | | | Water | 0·0 | | −10·9 |

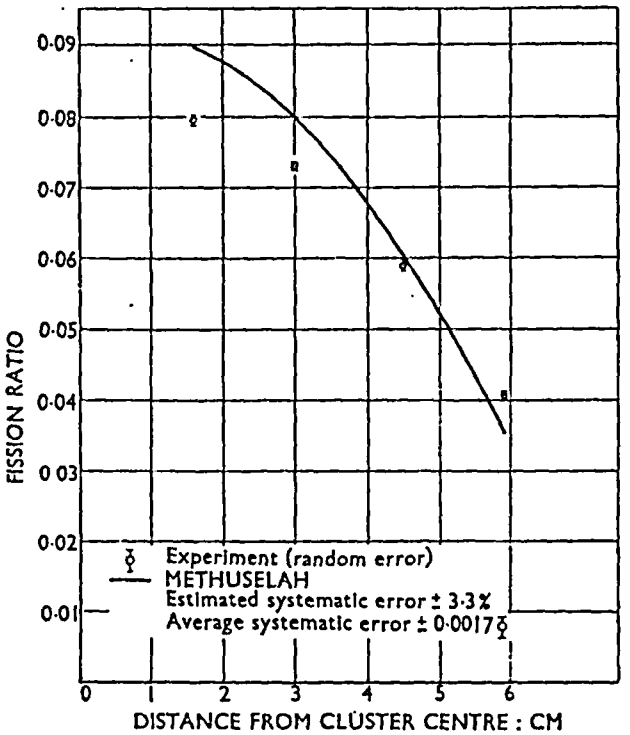


*Fig 4* **Fast fission rate distribution in core SG19 (water)**

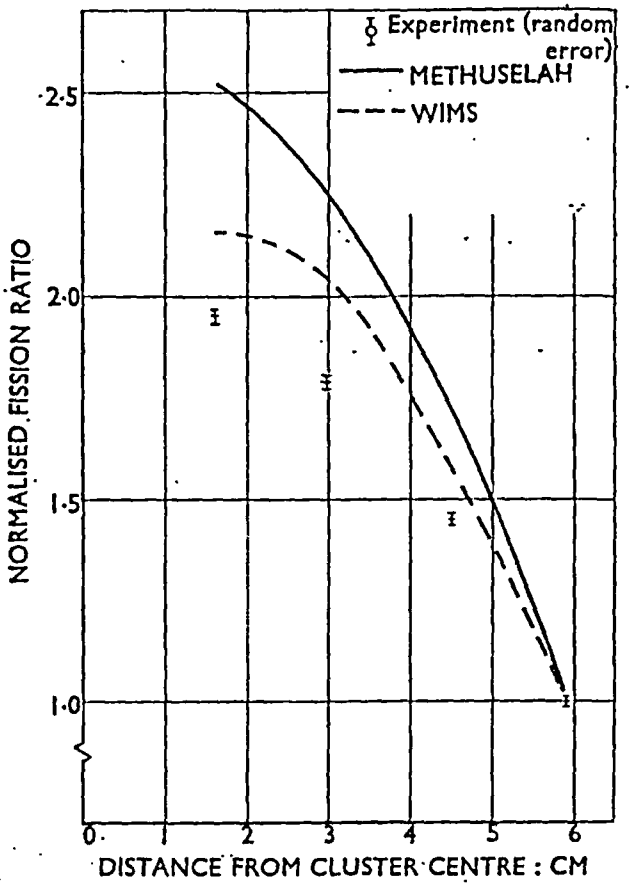


*Fig 5* **Normalized fast fission ratio distribution in core SG19 (water)**

*Radial distributions across cluster*

The measured distribution of fission ratio across a typical cluster are compared with the METHUSELAH predictions in Fig. 4. The fission ratio in the central pin in this and in some of the other cores is significantly overestimated. The reason for this becomes apparent on inspection of the approximate volumes of coolant associated with individual pins in successive rings of fuel as shown in Table 5. (See discussion of choice of ring boundaries in para. 64.)

55. In core SG19 the amount of coolant associated with the central pin is significantly larger than for the adjoining pins and the use of diffusion theory in METHUSELAH is inadequate to deal with this type of local effect, although its influence on the cluster average value is negligible as shown by the good agreement in Table 4. It would be anticipated that the use of transport theory in WIMS would lead to a more accurate prediction of the cluster distribution, and this is shown to be the case in Fig. 5 where the METHUSELAH and WIMS predictions are compared with experimental values of fission ratio normalized to unity in the outer ring of fuel. The measured rise of 95% is overestimated by 55% by METHUSELAH but only by 20% by WIMS. The WIMS results quoted here also involve ring smearing but with a somewhat different choice of ring boundaries from METHUSELAH. (See para. 68.)

56. Since the measured quantity is the ratio between U-238 and U-235 fissions, there remains the question of whether the discrepancies noted in clusters containing additional moderator near the centre pin are due to errors in predicting fast or thermal events. The illustrations in references 15 and 16 show that both METHUSELAH and WIMS predict U-235 fission rate distributions across SGHW clusters with good accuracy. In particular, in the SG19/Water core, both theories predict the measured maximum/minimum fission rate ratio to within 10%. Since any correction applied to the calculated U-235 fission rate

**Table 5:** *Volumes of coolant associated with unit volume of fuel pin in METHUSELAH*

| Core | Content of centre pin | Fuel ring | | | | | |
|---|---|---|---|---|---|---|---|
| | | 1 | 2 | 3 | 4 | 5 | 6 |
| SG1 | Stainless steel | 0·98 | 1·97 | 1·77 | 1·74 | 1·71 | 1·70 |
| SG2 | $UO_2$ | 1·43 | 1·46 | 1·29 | 1·46 | — | — |
| SG3, 4, 5 and 6 | $UO_2$ | 0·98 | 0·85 | 0·67 | 0·84 | — | — |
| SG12 | $UO_2$ | 1·35 | 1·07 | 1·09 | 1·02 | — | — |
| SG13 | $UO_2$ | 2·33 | 1·48 | 1·05 | 0·99 | 0·99 | — |
| SG19 | Air | 1·22 | 0·92 | 0·91 | 0·96 | 0·94 | — |
| SGP2 | Air | 1·21 | 0·91 | 0·90 | 0·95 | 0·92 | — |

The low coolant to fuel ratio in the third ring of the SG3, 4, 5 and 6 cores is a result of the three aluminium support tubes displacing coolant.

distribution will imply a corresponding correction in the same sense to the distribution of U-238 fission, it is clear that errors in the prediction of thermal fine structure cannot alone account for the observed discrepancies in FR distribution.

### Relative conversion ratio

*Cluster average values*

The measured cluster average values of relative conversion ratio are compared with the METHUSELAH predictions in Table 6. Measurements in individual pin positions are tabulated in reference 15, coincidence and chemistry determinations being listed separately. A number of small corrections are applied to the raw RCR results in Table 6 to obtain the values for direct comparison with theory. These cover the breakthrough of fission products and the increased efficiency of foil edge counting during coincidence counting, and have been discussed in paras 20–22. Other corrections arise because of small differences in diameter and oxide density between the standard fuel pins and the special demountable pins used for the measurements of fast fission and relative conversion ratio, but these have been shown to be negligible in para. 50.

58. The U-238 resonance data used in the METHUSELAH resonance group 3 are based on resonance integrals from Hellstrand's single rod measurements.[29] METHUSELAH modifies the resonance integrals to take account of the Dancoff effect which varies according to the position of the pin in the cluster. The distortion in the shape of the group 3 flux across the cluster is also estimated in forming the cross-sections. This treatment of resonance capture has improved the prediction of relative conversion ratio. Omitting core SGP2 which seems to be anomalous, the average discrepancy for the liquid cooled cores is −0·7% compared with −1·2% in METHUSELAH I, which was based on Hellstrand's measurements of resonance capture in rod clusters.[30] For the air cooled cores, too, there is a significant improvement, the average discrepancy being reduced from −4·9% to −1·8%. In the case of the plutonium fuelled core, SGP2, METHUSELAH gives a significantly larger underestimate than in any of the uranium fuelled cores. This result may be anomalous, but the consistency of the WIMS underestimate for all the mixture cooled cores implies that the METHUSELAH prediction may be at fault in this case.

59. Even at the WIMS level of sophistication some approximations are still necessary in representing the neutron processes, but many theoretical checks on the reliability of these approximations have been made, particularly in the resonance treatment,[33] and some confidence exists that the level of calculation should now be adequate to make quantitative inferences in the adequacy of fundamental nuclear data. As a result of a wide survey of reported lattice experiments using an earlier version of the WIMS code and data based on the UKAEA Nuclear Data Library,[30] Askew has proposed[34] a modification to the U-238 resonance data which is equivalent to an 8% reduction for a 1 cm diameter $UO_2$ pin in a 1:1 light water lattice and a 12% reduction for a metal pin in the same lattice. All

Table 6: *Cluster average values of relative conversion ratio (RCR)*

| | | Relative conversion ratio | | | | | | | | | | |
|---|---|---|---|---|---|---|---|---|---|---|---|---|
| | | | Corrections % | | | Experiment (corrected) | Random error % | Systematic error % | METHUSELAH II | Discrepancy % | WIMS | Discrepancy % |
| Core | Coolant | Expt. | $Q(t)$ | Edge | Total | | | | | | | |
| SG1 | Air | 2·134 | +0·3 | −0·2 | +0·1 | 2·136 | ±0·7 | ±0·7 | 2·089 | −2·2 | 2·101 | −1·7 |
| SG1 | Water | 1·690 | +0·3 | −0·2 | +0·1 | 1·692 | ±1·6 | ±0·7 | 1·675 | −1·0 | 1·663 | −1·8 |
| SG2 | Air | 2·012 | +0·4 | −0·2 | +0·2 | 2·016 | ±1·0 | ±0·7 | 1·966 | −2·5 | | |
| SG3 | Air | 1·983 | +0·4 | −0·2 | +0·2 | 1·987 | ±0·5 | ±0·7 | 1·967 | −1·0 | 1·917 | −3·5 |
| SG3 | Mixture | 1·890 | +0·4 | −0·2 | +0·2 | 1·894 | ±0·7 | ±0·7 | 1·882 | −0·6 | 1·834 | −3·2 |
| SG3 | Beads | 1·817 | +0·4 | −0·2 | +0·2 | 1·821 | ±0·7 | ±0·7 | 1·829 | +0·5 | | |
| SG3 | Water | 1·704 | +0·4 | −0·2 | +0·2 | 1·707 | ±0·8 | ±0·7 | 1·691 | −1·0 | 1·670 | −2·2 |
| SG3 | Water 90°C | 1·717 | +0·4 | −0·2 | +0·2 | 1·720 | ±1·3 | ±0·7 | 1·723 | +0·2 | | |
| SG4 | Mixture | 1·818 | +0·4 | −0·2 | +0·2 | 1·822 | ±0·7 | ±0·7 | 1·808 | −0·7 | 1·767 | −3·0 |
| SG4 | Water | 1·653 | +0·4 | −0·2 | +0·2 | 1·656 | ±1·3 | ±0·7 | 1·649 | −0·4 | 1·630 | −1·7 |
| SG5 | Mixture | 1·881 | +0·4 | −0·2 | +0·2 | 1·885 | ±1·0 | ±0·7 | 1·903 | +0·9 | | |
| SG5 | Water | 1·703 | +0·4 | −0·2 | +0·2 | 1·706 | ±1·1 | ±0·7 | 1·706 | 0·0 | | |
| SG6 | Mixture | 1·888 | +0·4 | −0·2 | +0·2 | 1·892 | ±0·6 | ±0·7 | 1·908 | +0·8 | | |
| SG6 | Water | 1·705 | +0·4 | −0·2 | +0·2 | 1·708 | ±0·5 | ±0·7 | 1·708 | 0·0 | | |
| SG12 | Mixture | 2·273 | +0·6 | −0·2 | +0·4 | 2·282 | ±0·5 | ±0·7 | 2·219 | −2·8 | 2·190 | −4·0 |
| SG12 | Water | 1·980 | +0·6 | −0·2 | +0·4 | 1·988 | ±0·4 | ±0·7 | 1·958 | −1·5 | 1·962 | −1·3 |
| SG13 | Air | 2·278 | +0·4 | −0·2 | +0·2 | 2·283 | ±0·7 | ±0·7 | 2·250 | −1·4 | 2·206 | −3·5 |
| SG13 | Mixture | 2·195 | +0·4 | −0·2 | +0·2 | 2·199 | ±0·4 | ±0·7 | 2·163 | −1·7 | 2·129 | −3·2 |
| SG13 | Water | 1·883 | +0·4 | −0·2 | +0·2 | 1·887 | ±0·4 | ±0·7 | 1·879 | −0·4 | 1·881 | −0·4 |
| SG19 | Water | 1·922 | +0·4 | — | +0·4 | 1·930 | ±0·9 | ±0·7 | 1·914 | −0·8 | 1·901 | −1·5 |
| SGP2 | Mixture | 2·512 | +0·6 | — | +0·6 | 2·527 | ±0·9 | ±0·7 | 2·411 | −4·6 | 2·425 | −4·0 |
| | | | | | | *Average discrepancies:* | | Air | | −1·8 | | −2·9 |
| | | | | | | | | Mixture | | −1·2* | | −3·5 |
| | | | | | | | | Water | | −0·6 | | −1·5 |

*the plutonium fuelled core, SGP2 is excluded the average for the uranium fuelled cores is −0·7%.

of the WIMS results presented here have used these modified U-238 data, together with U-235 data having an α-value of 0·5 above 0·5 eV. Previous comparisons with THULE predictions for liquid cooled SGHW clusters provided additional evidence of the need for modified U-238 data as discussed in para. 27.

60. More recent evidence suggests that the above modification is a slight over-correction and this view is supported by the figures in Table 6. The measured RCR is underestimated by WIMS by 1·5% for water cooled cores and by 3·5% for mixture cooled cores. Pending revisions to the UKAEA Nuclear Data File for deuterium suggest that the trend with coolant will be reduced but there is still a suggestion that the modification proposed by Askew may be a slight over-correction for these lattices. This point is discussed in reference 16.

*Radial distributions across cluster*

Cluster distributions of relative conversion ratio are compared with the METHUSELAH predictions in reference

Table 7: *Maximum/average values of manganese reaction rate ratio*

| | | Maximum/average reaction rate ratio | | | | | | |
|---|---|---|---|---|---|---|---|---|
| Core | Coolant | Expt. | Random error % | Systematic error % | METHUSELAH II | Discrepancy % | WIMS | Discrepancy % |
| SG1 | Air | 1·115 | ±2·0 | ±0·3 | 1·111 | −0·5 | 1·117 | +0·2 |
| SG1 | Water | 1·206 | ±2·0 | ±0·3 | 1·234 | +2·3 | 1·214 | +0·7 |
| SG3 | Air | 1·118 | ±2·0 | ±0·3 | 1·108 | −0·9 | 1·105 | −1·2 |
| SG3 | Mixture | 1·153 | ±2·0 | ±0·3 | 1·166 | +1·1 | 1·161 | +0·7 |
| SG3 | Beads | 1·169 | ±2·0 | ±0·3 | 1·160 | −0·8 | | |
| SG3 | Water | 1·201 | ±2·0 | ±0·3 | 1·186 | −1·2 | 1·197 | −0·3 |
| SG3 | Warm Water | 1·181 | ±2·0 | ±0·3 | 1·182 | +0·1 | | |
| SG4 | Mixture | 1·170 | ±0·5 | ±0·3 | 1·167 | −0·3 | 1·167 | −0·3 |
| SG4 | Water | 1·200 | ±0·5 | ±0·3 | 1·195 | −0·4 | 1·206 | +0·5 |
| SG5 | Mixture | 1·156 | ±0·5 | ±0·3 | 1·157 | +0·1 | | |
| SG5 | Water | 1·200 | ±0·5 | ±0·3 | 1·180 | −1·7 | | |
| SG6 | Mixture | 1·179 | ±0·5 | ±0·3 | 1·157 | −1·9 | | |
| SG6 | Water | 1·192 | ±0·5 | ±0·3 | 1·179 | −1·1 | | |
| SG11 | Air | 1·145 | ±1·8 | ±0·3 | 1·166 | +1·8 | 1·156 | +1·0 |
| SG11 | Water | 1·214 | ±0·9 | ±0·3 | 1·310 | +6·1 | 1·289 | +6·2 |
| SG12 | Mixture | 1·246 | ±0·3 | ±0·3 | 1·256 | +0·8 | 1·254 | +0·6 |
| SG12 | Water | 1·275 | ±0·4 | ±0·3 | 1·305 | +2·4 | 1·303 | +2·2 |
| SG13 | Air | 1·170 | ±0·4 | ±0·3 | 1·179 | +0·8 | 1·160 | −0·9 |
| SG13 | Mixture | 1·214 | ±0·4 | ±0·3 | 1·250 | +3·0 | 1·230 | +1·3 |
| SG13 | Water | 1·199 | ±0·6 | ±0·3 | 1·266 | +5·6 | 1·253 | +4·5 |
| SG15/E | Mixture* | 1·218 | ±0·3 | ±0·3 | 1·257 | +3·4 | | |
| SG15/E | Water* | 1·200 | ±0·3 | ±0·3 | 1·269 | +5·7 | | |
| SG15/F | Mixture | 1·250 | ±0·3 | ±0·3 | 1·286 | +2·6 | 1·257 | +0·6 |
| SG15/F | Water | 1·241 | ±0·3 | ±0·3 | 1·308 | +5·4 | 1·279 | +3·1 |
| | | | | *Average discrepancies:* | Air | +0·3 | | −0·3 |
| | | | | | Mixture | +1·2 | | +0·6 |
| | | | | | Water | +1·9 | | +2·4 |

* The displacement tubes were empty in these cores and full in the following two cores.

Table 8: *Maximum/average values of U-235 fission rate ratio*

| | | Maximum/average fission rate ratio | | | | | | |
|---|---|---|---|---|---|---|---|---|
| Core | Coolant | Expt. | Random error % | Systematic error % | METHUSELAH II | Discrepancy % | WIMS | Discrepancy % |
| SG17($B_0$) | Mixture | 1·265 | ±1·0 | ±0·2 | 1·314 | +2·9 | 1·284 | +1·5 |
| SG19 | Mixture | 1·274 | ±1·2 | ±0·2 | 1·314 | +3·2 | 1·292 | +1·4 |
| SG19 | Water | 1·256 | ±0·6 | ±0·2 | 1·328 | +5·7 | 1·304 | +3·8 |
| SGP1 | Mixture | 1·267 | ±1·2 | ±0·2 | 1·331 | +5·1 | 1·297 | +2·4 |
| SGP1 | Water | 1·265 | ±0·8 | ±0·2 | 1·340 | +5·9 | 1·317 | +4·1 |
| SGP2 | Mixture | 1·318 | ±2·5 | ±0·2 | 1·398 | +6·1 | 1·364 | +3·5 |
| SGP2 | Water | 1·307 | ±0·6 | ±0·2 | 1·392 | +6·5 | 1·374 | +5·1 |
| | | | | *Average discrepancies:* | Mixture | +4·3 | | +2·2 |
| | | | | | Water | +6·0 | | +4·3 |

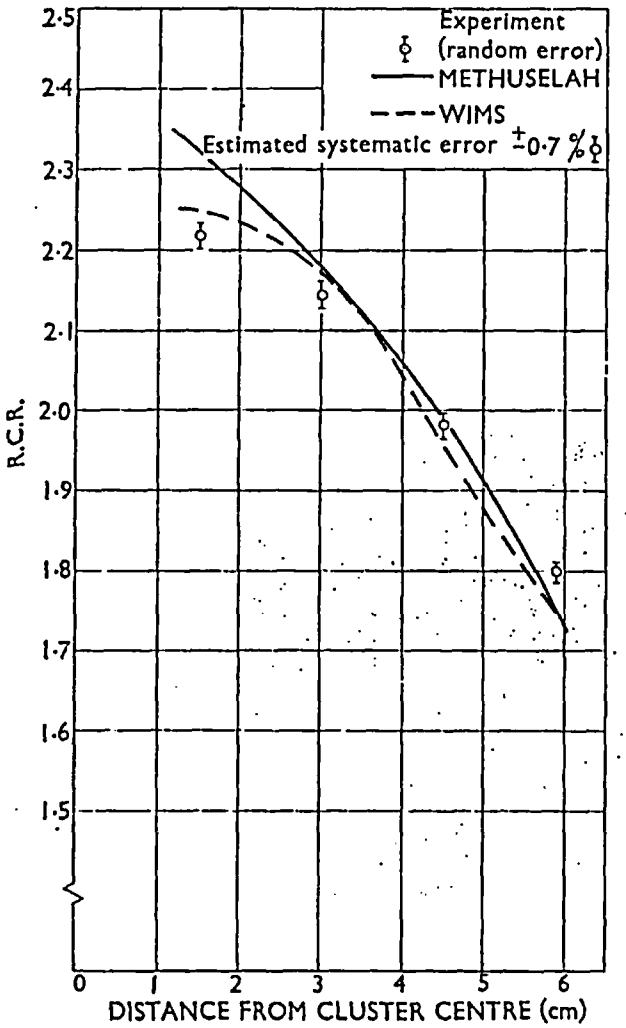


*Fig 6* **RCR distribution in core SG19 (water)**

15 and a typical example is shown in Fig. 6. In general, the agreement is good but there is the same tendency to overestimate near the centre of the liquid cooled clusters as was observed in the fission ratio comparison.

62. The WIMS resonance treatment involves the calculation of two Dancoff factors, one an average for all pins in the cluster and one for all pins except the outer ring. The difference is then ascribed to the outer ring only. Despite this discontinuity it will be seen that the WIMS ring by ring distribution agrees quite well with experiment, and, in particular, predicts the distribution near the centre of the cluster better than METHUSELAH.

### Thermal fine structure

Measurements of thermal fine structure have been made in most of the lattices listed in Table 1 using either manganese-nickel or uranium-nickel foils. Detailed results are given in reference 15 and typical cluster distributions are plotted in Figs 7 and 8. The relevant measuring techniques have been described in reference 6. Maximum/average reaction and fission rate ratios in each fuel cluster are compared with theory in Tables 7 and 8.

64. The METHUSELAH predictions of maximum/average manganese reaction and U-235 fission rates have been modified by the allowance for absorption hardening in the overlapping group scheme as discussed in para. 35. In ring smearing the fuel pins in a cluster, the coolant immediately adjoining the inside of the pressure tube can either be treated as a separate annular region or smeared in with the outer ring of pins. Comparisons have shown that the former convention yields better results and this method has therefore been adopted for all METHUSELAH calculations. METHUSELAH calculates the positions of the boundaries between fuel rings from the input cluster geometry using a simple prescription.[11] In these calculations the outer boundary of the cluster was defined by making the ratio of volume of coolant to volume of fuel in the outer ring equal to the ratio in the penultimate ring.

65. These changes have led to a much more consistent performance. In the SG1, SG13 and subsequent cores which used fairly uniform multi-rod clusters (see Fig. 2), the METHUSELAH predictions of maximum/average ratios in the water and mixture cores are consistently high by a few per cent. The average overestimates in these cores are $4 \pm 1\%$ with mixture coolant and $5 \pm 1\%$ with water coolant. Since diffusion theory is used with basic thermal nuclear data, closer agreement between theory and experiment is not to be expected, but the consistency of the results is most encouraging and shows that METHUSELAH predictions of cluster power distribution in these cores will include a small safety margin. The SG3–SG6 cores all used the same rather irregular 37 pin cluster shown in Fig. 1 and in these cases the average METHUSELAH discrepancy is only $-0{\cdot}6\%$.

66. Measurements of the manganese reaction rate were also made on the pressure and calandria tubes and into the $D_2O$ bulk moderator as described in reference 6. In most cases, measurements were made along two axes, viz. the 'short' axis towards an adjacent cluster, and the 'long' axis towards the space between two adjoining clusters. Both sets of experimental points are plotted in Figs 7 and 8, and the mean values are then compared with the theoretical predictions based on a cylindrical cell approximation. Small negative corrections (of about $-1{\cdot}5\%$) have been applied to the measurements made in the moderator to allow for the difference in the importance of resonance self-shielding between the moderator and fuel regions as discussed in reference 5.

67. The shape of the thermal fine structure outside the fuel cluster is in reasonable agreement with the measurements. For mixture and water cooled cores, mean reaction rates in the pressure tube, calandria tube and moderator relative to the fuel are generally calculated to within $\pm 5\%$. Larger discrepancies occur in the corners of square unit cells where the approximations of cylindricalization become poor, but these are of limited significance. For the uranium fuelled cores, the slight trend for METHUSELAH to overestimate the increase of fine structure with increasing effective coolant density remains, but it is reduced in the cores which contain plutonium.

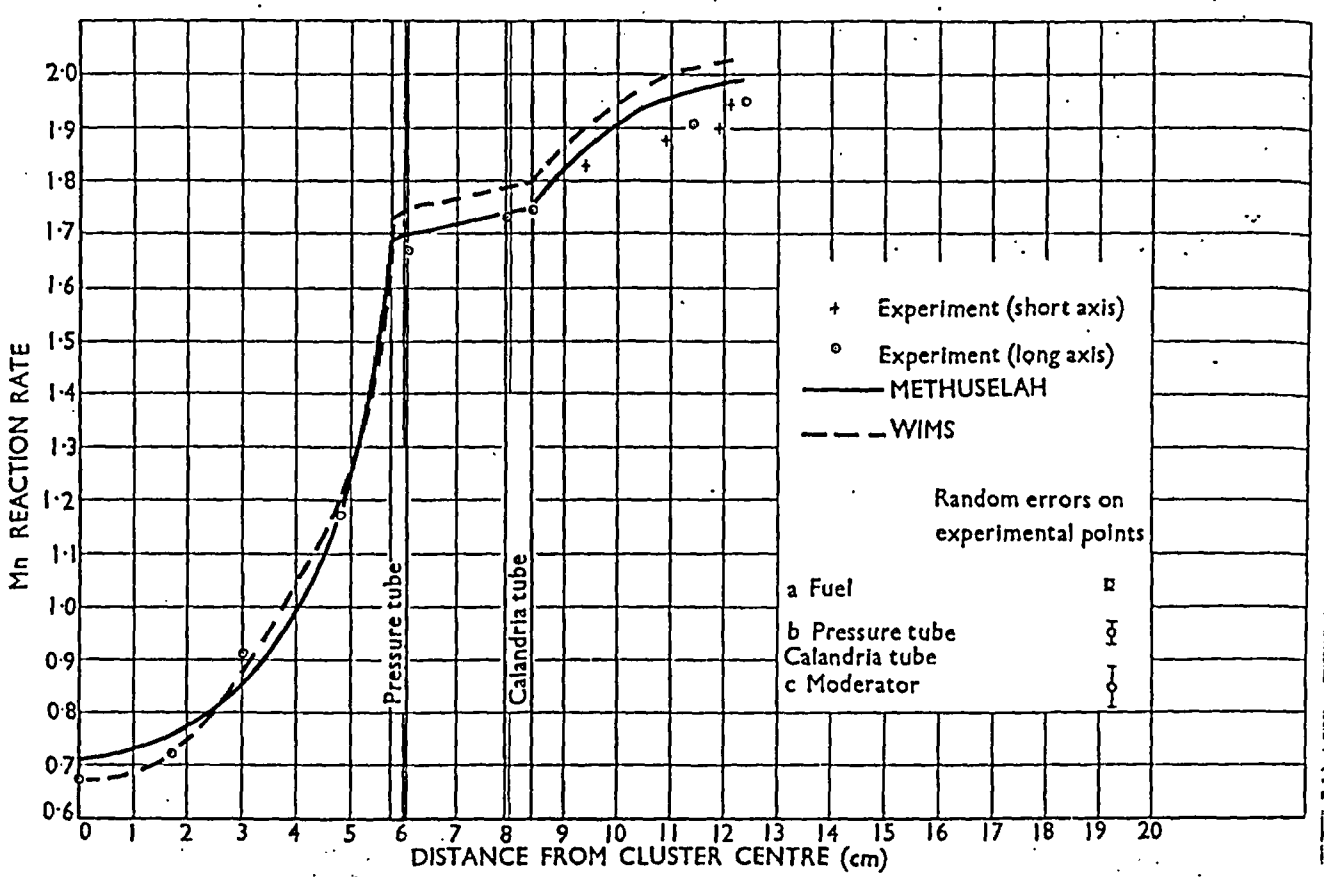


*Fig 7* **Manganese reaction rate distribution in core SG3 (water)**

68. Like METHUSELAH, the option of WIMS used for these results has employed a ring-smearing model but the boundaries have been chosen on a somewhat different basis. Smearing over an annulus means that the fissile isotopes are, in general, displaced radially with respect to the true pin geometry, which can lead to significant errors in the presence of steep radial flux gradients such as exist in these SGHW lattices. In order to minimize this effect, the ring boundaries are chosen so that the mean radial coordinate of the annular fuel smear is equal to that of the ring of fuel pins. The coolant/fuel volume ratio in the outer ring is made equal to that in the penultimate ring so that a water annulus adjoining the pressure tube is treated as a separate region as in METHUSELAH.

69. Results based on the PIJ option of WIMS, which can treat individual pins, will be reported in a later publication,[18] but even the WDSN option is seen to give good predictions of thermal fine structure. The predictions of maximum/average fine structure in the fuel are similar to those of METHUSELAH, the discrepancies being 3% high for water coolant, 1½% high for mixture coolant and vanishingly small for air coolant.

70. Examination of Figs 7 and 8 shows that, in these cases, WIMS predicts the shape of the curve near the inner pins rather more accurately than METHUSELAH. For water cooled cores the WIMS predictions of thermal fine structure outside the fuel cluster are similar to those of METHUSELAH being within about 5% of experiment. For mixture and air cooled cores, however, they are much more accurate.

### Hyperfine structure in the thermal flux distribution

A typical experimental arrangement for the measurement of thermal hyperfine structure is shown in Fig. 9; the details of the method are described in reference 42. Circular manganese–nickel foils of the same diameter as the fuel pellets are irradiated in each type of fuel pin; a variety of sector foils span the whole of the representative region of the coolant. Once the various foils have been intercalibrated, an average hyperfine structure factor for the whole cluster may be inferred.

72. Small perturbation effects are caused by the mismatch in absorption and slowing down power between the 0·005 in. manganese–nickel foils and the fuel or coolant in which they are placed. Since thermal hyperfine structure is relatively unimportant in SGHW lattices, these perturbation effects were not determined experimentally in every

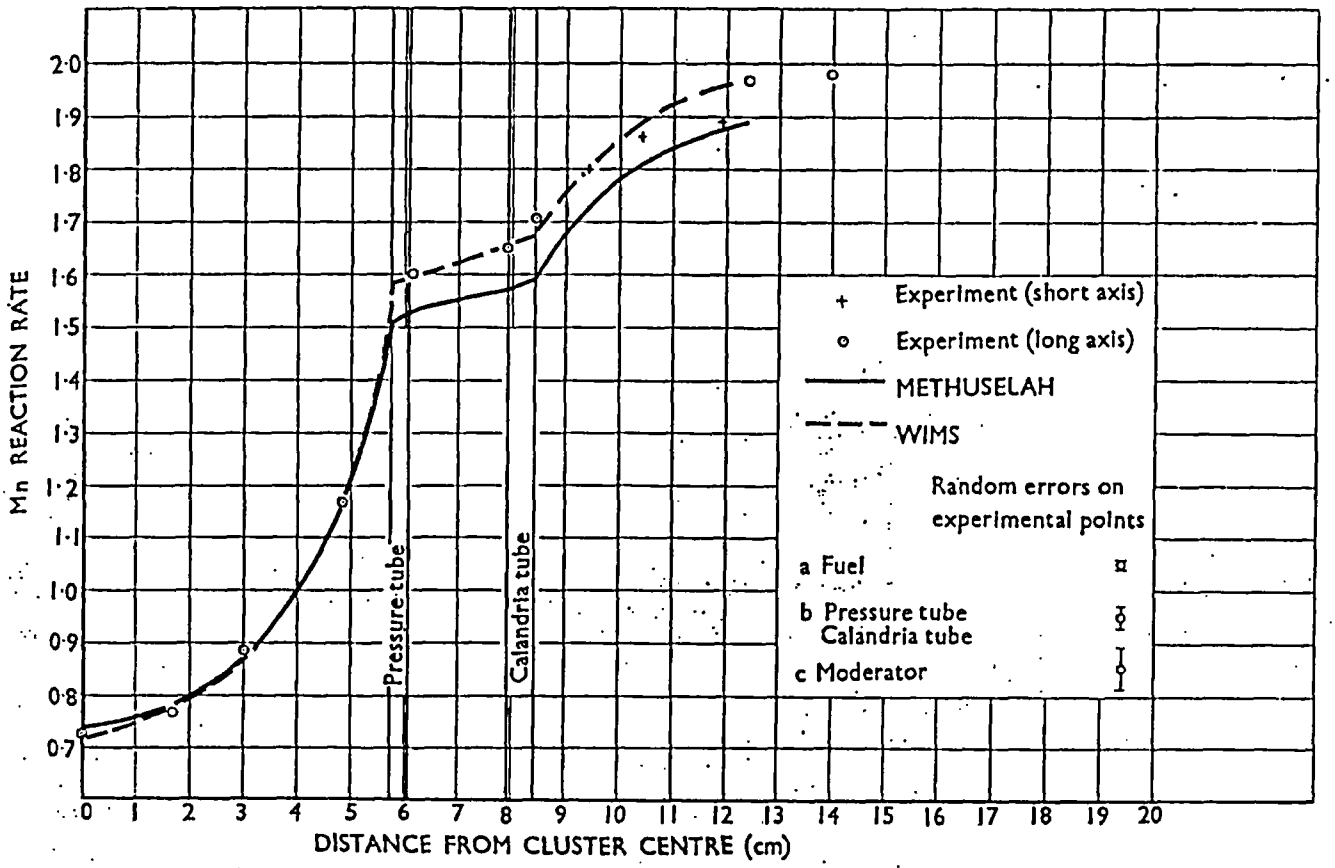


*Fig 8* Manganese reaction rate distribution in core SG3 (mixture)

core, but check measurements[42] showed that the differences between the perturbations in fuel and coolant should not exceed 1%. The systematic errors associated with the measurements have therefore been increased by this amount.

73. METHUSELAH uses hyperfine structure factors which are calculated separately for each ring of pins using collision theory and slab geometry; the hyperfine structure factors are calculated in infinite arrays of such cells. For comparison with the experimental hyperfine structure results, the ratio between the mean coolant flux and mean fuel flux is obtained by appropriate volume weighting of the calculated fluxes over the finite cluster. Measurements have been made in seven cores with the results listed in Table 9.

74. The agreement between METHUSELAH and experiment is good, the mean discrepancy being less than 1% for both water and mixture coolant. Since the method of calculating hyperfine structure has not changed, it is interesting that the changes in deriving the cross-sections in METHUSELAH have led to an improved calculation of hyperfine structure. The average discrepancies previously reported in reference 4 were 3·0% for mixture coolant falling to 1·8% for water coolant.

75. About 9% of the thermal neutrons are captured in

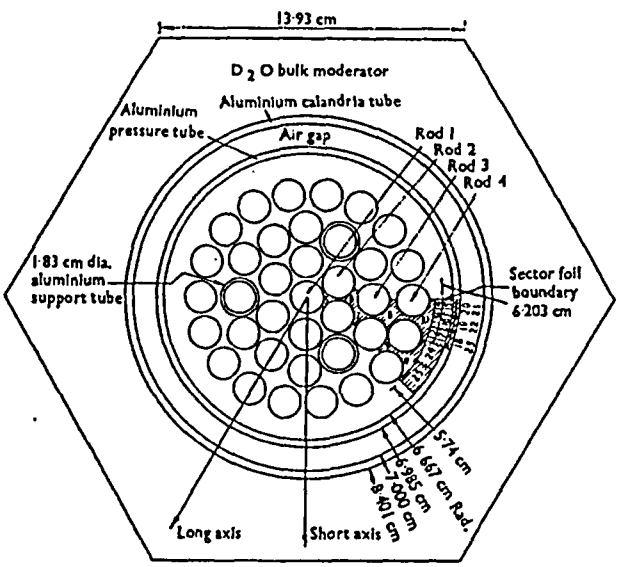


*Fig 9* Experimental arrangement for the measurement of hyperfine structure in core SG5

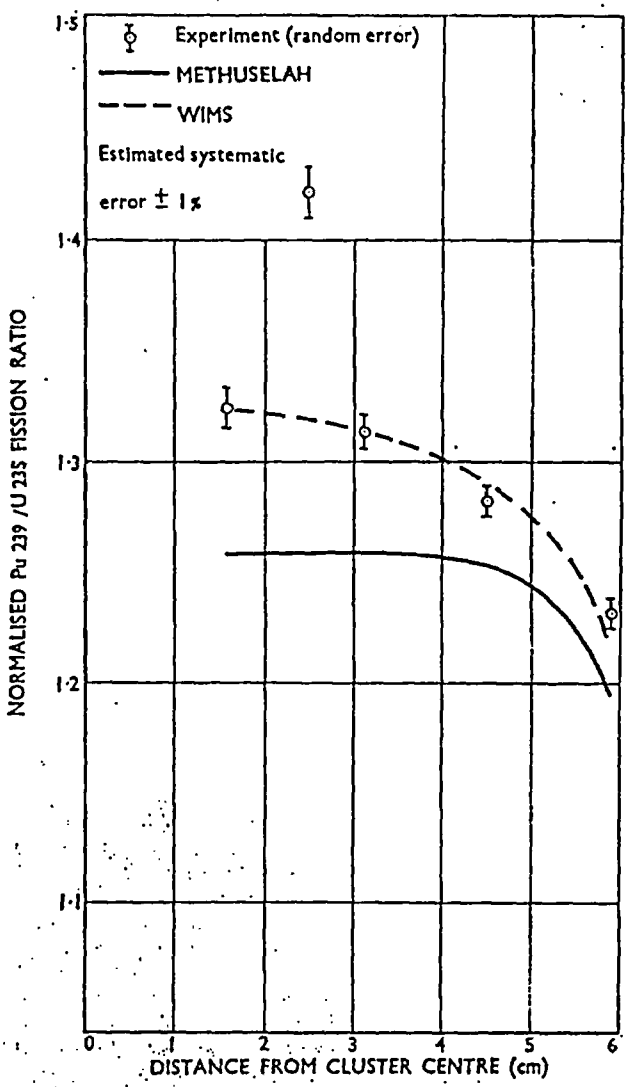


*Fig 10* Normalized $Pu^{239}/U^{235}$ fission ratio distribution in core SG19 (water)

the coolant of the light water coolant cores and about 3% are captured in the coolant of the mixture coolant cores. Thus, a 1% discrepancy in the hyperfine structure is worth about 0·1% and 0·03% in reactivity for these two coolant types respectively. There should be a hyperfine structure correction to $k$-inf when inferring $k$-inf (reaction rate) (see reference 20). However, as the hyperfine flux structure has not been measured in all cores, such an application would introduce an artificial trend in the results. In any case, the corrections are small and so have been ignored.

76. The limited number of WIMS results quoted show no trends. The r.m.s. discrepancy is slightly larger than that produced by METHUSELAH but still within the quoted experimental errors. Explicit collision probability (PIJ-WIMS) results[18] should help to evaluate any errors due to the hyperfine structure calculation model.

### Integral thermal neutron spectra

Predictions of cluster average values of plutonium/uranium fission rate and lutecium/manganese reaction rate ratios normalized to unity in a thermal spectrum are compared with the measured values in Tables 10 and 11. The results of measurements of detailed cluster distributions are compared with theoretical predictions in references 15 and 16.

78. The use of a gas model for $H_2O$ in METHUSELAH leads to a consistent tendency to predict too soft a spectrum and hence to underestimate both the plutonium/uranium and the lutecium/manganese ratios in the fuel region. In the case of the plutonium/uranium ratio, this is not immediately obvious from the cluster average values quoted in Table 10, but the typical detailed cluster distribution in Fig. 10 shows that there is a tendency to underestimate the plutonium/uranium ratio near the centre of liquid cooled clusters where the thermal spectrum would be expected to have reached a near asymptotic state. In almost every case, theory and experiment converge near the outer ring of fuel where the spectrum is dominated by the neutrons thermalized in the $D_2O$ moderator. Since the cluster average is dominated by the larger numbers of pins in the outer rings, a spuriously good agreement is obtained in Table 10. METHUSELAH calculates the mean thermal spectrum for the homogenized cluster, whereas the measurements were made in the fuel pins. WIMS calculates the

Table 9: *Cluster averaged hyperfine structure factors* $\frac{\phi_{coolant}}{\phi_{fuel}}$

| | | $\phi_{coolant}/\phi_{fuel}$ | | | | | | |
|---|---|---|---|---|---|---|---|---|
| Core | Coolant | Expt. | Random error % | Systematic error % | METHUSELAH II | Discrepancy % | WIMS | Discrepancy % |
| SG3 | Mixture | 1·118 | ±1·8 | ±2·0 | 1·127 | +0·8 | 1·117 | −0·9 |
| SG3 | Beads | 1·151 | ±1·8 | ±2·0 | 1·135 | −1·4 | | |
| SG3 | Water | 1·176 | ±1·2 | ±2·0 | 1·163 | −1·1 | 1·209 | +2·8 |
| SG5 | Mixture | 1·141 | ±0·6 | ±2·0 | 1·124 | −1·5 | | |
| SG5 | Water | 1·157 | ±0·6 | ±2·0 | 1·160 | +0·3 | | |
| SG13 | Mixture | 1·105 | ±0·6 | ±2·0 | 1·089 | −1·4 | 1·126 | +1·9 |
| SG13 | Water | 1·179 | ±0·6 | ±2·0 | 1·121 | −0·7 | 1·158 | −1·8 |
| | | | | *Average discrepancies:* | Mixture | −0·7 | | +0·5 |
| | | | | | Water | −0·5 | | +0·5 |

spectra in fuel and coolant separately and is therefore free from this source of error. Check calculations using WIMS indicate that the use of a mean thermal spectrum in METHUSELAH is likely to lead to underestimates of 1 to 2% in the ratios measured in the fuel pins.

79. The lutecium/manganese reaction ratio is significantly underestimated throughout the fuel region, thus confirming the common observation that when a Wigner-Wilkins spectrum is used, the lutecium cross-section is relatively insensitive to absorption hardening.

80. The SPECTROX method[39] employed in WIMS allows for the influence of spatial coupling on the spectra of moderator, coolant, clad and fuel. These 69 group spectra are meant to be average spectra for fuel, etc., but

Table 10: *Normalized cluster average values of plutonium/uranium fission ratio*

| | | Plutonium/uranium fission ratio | | | | | | |
|---|---|---|---|---|---|---|---|---|
| Core | Coolant | Expt. | Random error % | Systematic error % | METHUSELAH II | Discrepancy % | WIMS | Discrepancy % |
| SG3 | Air | 1·350 | ±1·5 | ±1·0 | 1·316 | −2·5 | 1·373 | +1·7 |
| SG3 | Mixture | 1·270 | ±0·8 | ±1·0 | 1·289 | +1·5 | 1·285 | +1·1 |
| SG3 | Beads | 1·260 | ±0·8 | ±1·0 | 1·220 | −3·2 | | |
| SG3 | Water | 1·210 | ±0·8 | ±1·0 | 1·192 | −1·5 | 1·217 | +0·6 |
| SG3 | Warm Water | 1·290 | ±0·8 | ±1·0 | 1·252 | −2·9 | | |
| SG4 | Mixture | 1·280 | ±1·6 | ±1·0 | 1·286 | +0·5 | 1·266 | −1·1 |
| SG5 | Mixture | 1·250 | ±1·6 | ±1·0 | 1·295 | +3·6 | | |
| SG5 | Water | 1·190 | ±0·8 | ±1·0 | 1·195 | +0·4 | | |
| SG6 | Water | 1·170 | ±2·5 | ±1·0 | 1·196 | +2·2 | | |
| SG12 | Mixture | 1·280 | ±2·3 | ±1·0 | 1·305 | +2·0 | 1·309 | +2·3 |
| SG12 | Water | 1·220 | ±4·9 | ±1·0 | 1·194 | −2·1 | 1·223 | +0·2 |
| SG13 | Mixture | 1·280 | ±1·6 | ±1·0 | 1·320 | +3·1 | 1·326 | +3·6 |
| SG13 | Water | 1·230 | ±1·6 | ±1·0 | 1·206 | −2·0 | 1·246 | +1·3 |
| SG19 | Mixture | 1·302 | ±0·7 | ±1·0 | 1·323 | +1·6 | 1·300 | −0·2 |
| SG19 | Water | 1·265 | ±0·7 | ±1·0 | 1·224 | −3·2 | 1·254 | −0·9 |
| SGP1 | Mixture | 1·248 | ±0·4 | ±1·0 | 1·279 | +2·5 | 1·257 | +0·7 |
| SGP1 | Water | 1·232 | ±0·4 | ±1·0 | 1·195 | −3·0 | 1·214 | −1·5 |
| SGP2 | Mixture | 1·206 | ±0·4 | ±1·0 | 1·234 | +2·3 | 1·208 | +0·2 |
| SGP2 | Water | 1·211 | ±0·4 | ±1·0 | 1·191 | −1·7 | 1·193 | −1·5 |
| | | | | *Average discrepancies:* | Mixture | +2·1 | | +0·9 |
| | | | | | Water | −1·4 | | −0·3 |

Table 11: *Normalized cluster average values of lutecium/manganese reaction rate ratio*

| | | Lutecium/manganese reaction rate ratio | | | | | | |
|---|---|---|---|---|---|---|---|---|
| Core | Coolant | Expt. | Random error % | Systematic error % | METHUSELAH II | Discrepancy % | WIMS | Discrepancy % |
| SG3 | Air | 1·260 | ±0·8 | ±2·0 | 1·108 | −12·1 | 1·285 | −0·2 |
| SG3 | Beads | 1·230 | ±0·8 | ±2·0 | 1·127 | − 8·4 | | |
| SG3 | Water | 1·170 | ±1·7 | ±2·0 | 1·094 | − 6·5 | 1·167 | −0·3 |
| SG3 | Warm Water | 1·320 | ±1·5 | ±2·0 | 1·277 | − 3·3 | | |
| SG4 | Mixture | 1·220 | ±0·8 | ±2·0 | 1·145 | − 6·1 | 1·207 | −1·1 |
| SG4 | Water | 1·160 | ±0·9 | ±2·0 | 1·098 | − 5·3 | 1·166 | +0·5 |
| SG5 | Mixture | 1·240 | ±1·6 | ±2·0 | 1·142 | − 7·9 | | |
| SG5 | Water | 1·210 | ±1·7 | ±2·0 | 1·095 | − 9·5 | | |
| SG6 | Water | 1·210 | ±2·5 | ±2·0 | 1·095 | − 9·5 | | |
| SG12 | Mixture | 1·160 | ±0·9 | +2·0 | 1·140 | − 1·7 | 1·199 | +3·4 |
| SG12 | Water | 1·130 | ±0·9 | ±2·0 | 1·091 | − 3·5 | 1·168 | +3·4 |
| SG13 | Air | 1·260 | ±0·8 | ±2·0 | 1·082 | −14·1 | 1·253 | −0·6 |
| SG13 | Mixture | 1·200 | ±0·8 | ±2·0 | 1·137 | − 5·3 | 1·201 | +0·1 |
| SG13 | Water | 1·150 | ±0·9 | ±2·0 | 1·091 | − 5·1 | 1·168 | +1·6 |
| SG19 | Mixture | 1·181 | ±0·4 | ±2·0 | 1·138 | − 3·6 | 1·191 | +0·8 |
| SG19 | Water | 1·167 | ±0·4 | ±2·0 | 1·102 | − 5·5 | 1·171 | +0·3 |
| SGP1 | Mixture | 1·123 | ±0·4 | ±2·0 | 1·114 | − 0·8 | 1·166 | +3·8 |
| SGP1 | Water | 1·160 | ±0·4 | ±2·0 | 1·082 | − 6·6 | 1·149 | −1·0 |
| SGP2 | Mixture | 1·115 | ±0·4 | ±2·0 | 1·076 | − 3·4 | 1·115 | 0·0 |
| SGP2 | Water | 1·228 | ±0·4 | ±2·0 | 1·066 | −13·4 | 1·121 | −8·8 |
| | | | | *Average discrepancies:* | Mixture | − 4·1 | | +1·2 |
| | | | | | Water | − 7·2 | | −0·6 |

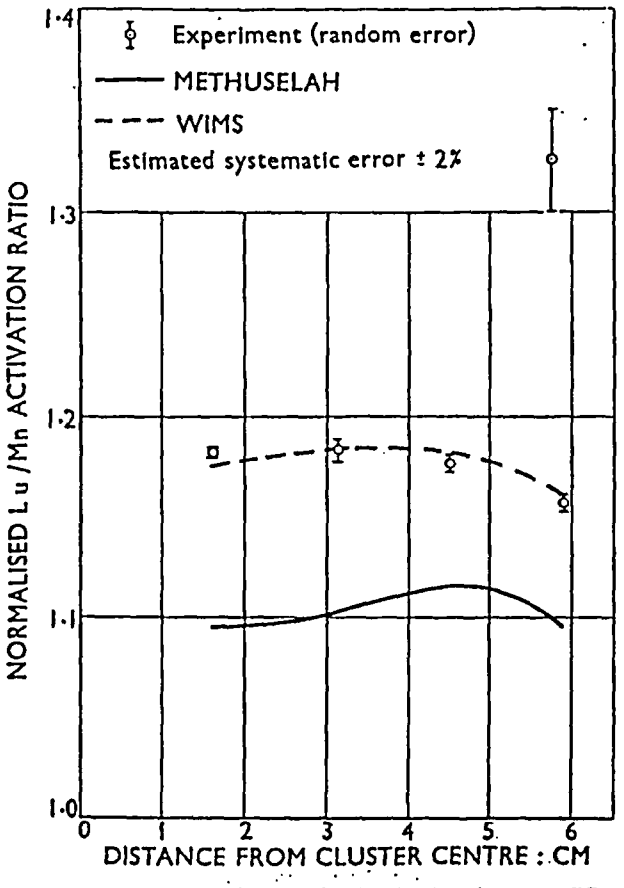


*Fig 11* Normalized Lu/Mn ratio distribution in core SG19 (water)

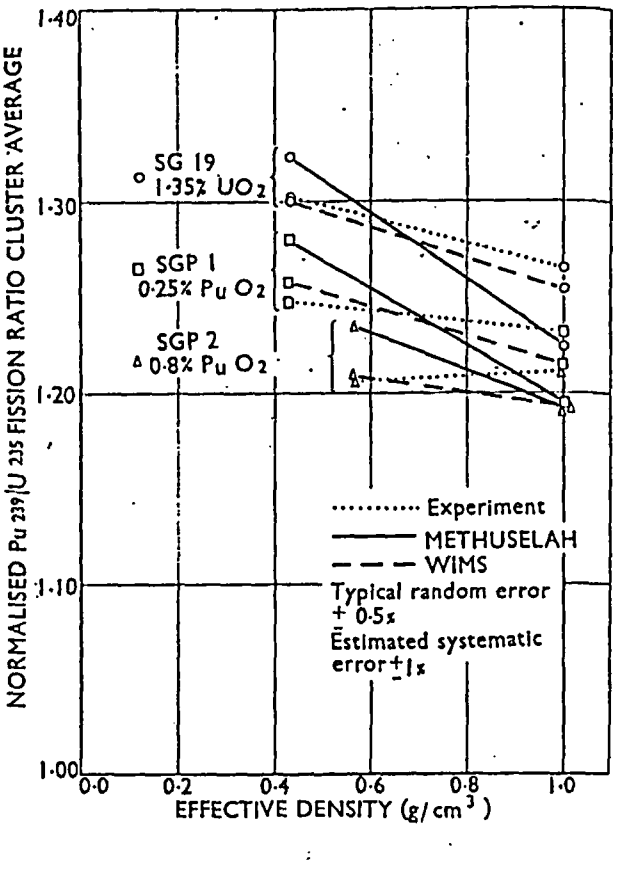


*Fig 12* Variation of $Pu^{239}/U^{235}$ fission ratio with effective coolant density

are used only for ring smearing and to condense the library data into fewer groups for the spatially detailed main transport solution. In these examples, 18 groups were used in the main flux solution, seven of them spanning the range 0·625 eV to zero and another three spanning the range from 0·625 eV to 4 eV.

81. Because of this detailed treatment and of the sophisticated scattering models in the data library in WIMS, one would expect improved predictions of integral neutron spectra and this is seen to be true in Tables 10 and 11, the predictions for the uranium fuelled cores being particularly good. The lutecium/manganese ratios are overestimated on average by 0·3% compared with the METHUSELAH underestimate of 5·6%. The cluster distributions, too, are more accurately predicted by WIMS as shown by the typical comparisons with experiment in Figs 10 and 11.

82. In a uranium fuelled core, the METHUSELAH tendency to predict too soft a spectrum is unimportant, but when a substantial fraction of the fissions occurs in plutonium fuel, an underestimate of the plutonium/uranium ratio by, say, 2% and of the lutecium/manganese ratio by 14% is equivalent to an underestimate of reactivity by 0·3% in a typical case; this discrepancy is small but it becomes more significant when calculating the void coefficient where a high degree of accuracy is required. This aspect is illustrated in Figs 12 and 13 where the calculated and measured values of the plutonium/uranium and lutecium/manganese ratios are shown as a function of effective coolant density for three oxide fuels differing only in their plutonium content. As the effective coolant density in a uranium fuelled core is decreased, the plutonium/uranium ratio increases. As uranium is replaced by plutonium, two main changes alter the shape of the thermal neutron spectrum, viz.:

(i) the higher thermal absorption of the plutonium causes some 'absorption hardening' of the spectrum, thus increasing the relative number of neutrons in the region of the 0·3 eV resonance;

(ii) the presence of plutonium atoms leads to depression in the neutron spectrum near 0·3 eV.

83. The experimental results shown in Fig. 12 suggest that the second effect is the dominating one, since the plutonium/uranium ratio at a given coolant density decreases as the proportion of plutonium increases, i.e. the flux depression effect is more than adequate to offset the

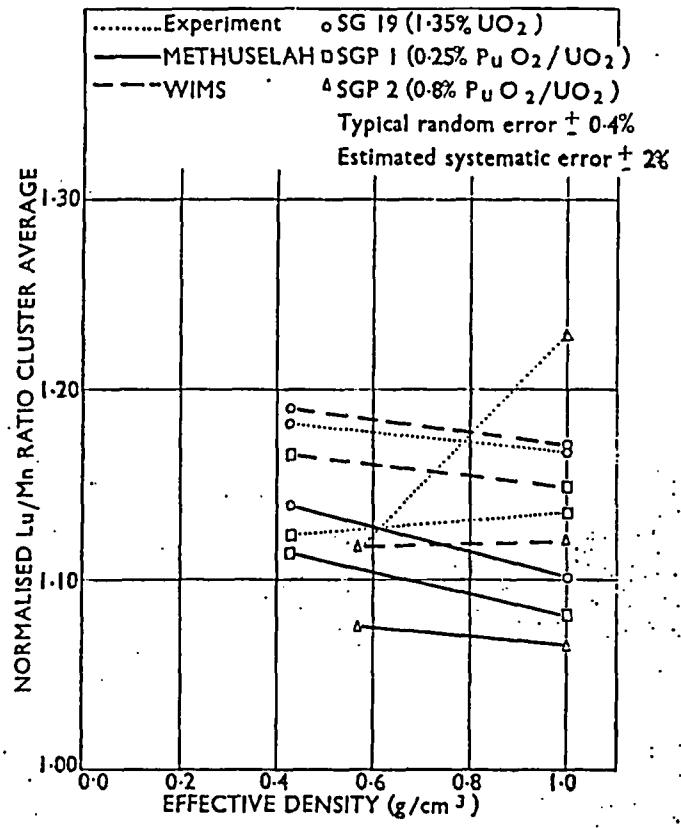


*Fig 13* Variation of Lu/Mn ratio with effective coolant density

rise in plutonium absorption cross-section associated with absorption hardening. This trend becomes more marked as the spectrum is hardened further by reducing the effective coolant density. The measured values for the lutecium/manganese ratios show a similar but larger trend with decreasing coolant density.

84. The rather simple spectrum model used in METHUSELAH would not be expected to predict complex phenomena of this kind, but the detailed representation of the spectrum in WIMS is ideally suited to this purpose. Figs 12 and 13 show that, although METHUSELAH predicts a flattening of the variation of spectral index with coolant density as plutonium is added to the core, the effects are considerably underestimated. In particular, with 0·8% $PuO_2/UO_2$ fuel, both plutonium/uranium and lutecium/manganese ratios increase with increasing coolant density whereas METHUSELAH predicts a decrease in both cases. WIMS predictions, based on a Nelkin scattering model for light water and a Honeck model for heavy water, are also plotted in the figures. Although some discrepancies remain, it is clear that the trends in the WIMS predictions are closer to the experimental values.

85. Since the above thermal spectrum discrepancies vary significantly with effective coolant density, their correction will affect the METHUSELAH predictions of void coefficient. This topic is discussed in para. 100; the effect of correcting for known errors in thermal spectrum predictions would make the predicted void coefficient in 0·8% $PuO_2/UO_2$ more negative by about 0·006. Since reactivity measurements have shown that the variation of void coefficient with the plutonium content of the fuel is predicted satisfactorily by METHUSELAH (see para. 100 and Fig. 17), some compensation of errors is clearly taking place.

## SURVEY OF EIGENVALUE AND *k*-INFINITY COMPARISONS

### Eigenvalues

Measurements of material buckling have been made in all the lattices listed in Table 1 with the exception of SG3 ('Beads') and SG19 (Mixture). In the earlier cores SG1–14, the measured bucklings include the effect of aluminium fuel cluster end fittings (see Table 1) and hence in computing the eigenvalue, corrections are required to both the reproduction constant and the leakage to allow for the presence of these fittings. In view of the decision to use continuous fuel in the later stages of the experimental programme and in the initial loading of the prototype SGHWR, a large investment of theoretical effort in this problem was not justified and the corrections have been made on a simple basis as described by Newmarch[43] and Terry.[12] An additional METHUSELAH option is provided which weights the cross-sections of the material of the end fittings by the unperturbed radial fluxes and the fractional volumes and then smears into the radial region of the cluster. For the sub-critical cores, these corrections vary from about 0·5% in the SG3/Air core to 2·0% for the SG3/Water core. The end plates are more widely spaced in the early critical cores SG11–14 but here, in some cases, an end fitting almost coincides with the peak of the macroscopic flux, thus making the buckling measurement uncertain as shown by the increased experimental errors associated with these measurements in Table 13.

87. The SG15, SG17, SG19, SGP1 and SGP2 cores do not have end fittings and thus, for these cores, the reactivities obtained from buckling measurements are much more accurate. Table 12 gives the values of *k*-eff inferred from the measured bucklings for the sub-critical cores, while Table 13 gives the values for the critical cores.

88. The METHUSELAH II eigenvalues are also plotted in Fig. 14 and some clear trends are observed. The 4% overestimate of reactivity by METHUSELAH I for air-cooled cores, attributed largely to the breakdown of the two overlapping thermal group models, has been reduced significantly, but the eigenvalues for these cores are still consistently high by about 2%. Among the liquid cooled cores, the early sub-critical lattices SG1–6 give accurate buckling measurements even though the fuel cluster end plates were present, because they were sufficiently large to allow measurements to be made at equivalent positions in the axial fine structure. The eigenvalues obtained for these cores are almost all within ±0·5% of unity which suggests that corrections of adequate accuracy have been applied for end plate effects.

89. In the early critical cores SG11–14, only one plane of cluster end plates was present in the central core region,

Table 12: *Bucklings and eigenvalues for the sub-critical cores*

| Core | Coolant | Buckling ($m^{-2}$) Radial | Buckling ($m^{-2}$) Axial | End fitting correction | *k*-eff Value | *k*-eff Random error % |
|---|---|---|---|---|---|---|
| SG1 | Air | 5·176±0·079 | −3·005±0·028 | +0·0106 | 1·0266 | ±0·0027 |
| SG1 | Water | 5·174±0·112 | −4·455±0·045 | +0·0245 | 1·0037 | ±0·0017 |
| SG2 | Air | 5·195±0·062 | −4·061±0·037 | +0·0090 | 1·0206 | ±0·0025 |
| SG2 | Water | 5·707±0·013 | −8·002±0·067 | +0·0228 | 0·9946 | ±0·0013 |
| SG3 | Air | 5·143±0·039 | −3·679±0·015 | +0·0052 | 1·0197 | ±0·0015 |
| SG3 | Mixture | 5·432±0·018 | −4·153±0·024 | +0·0137 | 1·0040 | ±0·0009 |
| SG3 | Water | 5·487±0·021 | −4·767±0·017 | +0·0184 | 0·9981 | ±0·0007 |
| SG4 | Air | 5·439±0·016 | −3·679±0·018 | +0·0088 | 1·0171 | ±0·0007 |
| SG4 | Mixture | 5·662±0·014 | −4·732±0·025 | +0·0161 | 1·0037 | ±0·0007 |
| SG4 | Water | 5·691±0·024 | −6·154±0·033 | +0·0194 | 1·0021 | ±0·0009 |
| SG5 | Air | 5·019±0·041 | −4·460±0·016 | +0·0073 | 1·0260 | ±0·0015 |
| SG5 | Mixture | 5·273±0·056 | −5·205±0·019 | +0·0158 | 1·0117 | ±0·0017 |
| SG5 | Water | 5·364±0·069 | −6·148±0·019 | +0·0204 | 1·0098 | ±0·0017 |
| SG6 | Air | 5·236±0·059 | −4·982±0·066 | +0·0075 | 1·0160 | ±0·0035 |
| SG6 | Mixture | 5·473±0·053 | −5·891±0·085 | +0·0158 | 1·0011 | ±0·0032 |
| SG6 | Water | 5·592±0·055 | −6·888±0·107 | +0·0204 | 0·9960 | ±0·0033 |
| | | | *Average values:* | Air | 1·0210 | |
| | | | | Mixture | 1·0051 | |
| | | | | Water | 1·0007 | |

*Note:* The estimated uncertainty in the calculated end plate corrections is ±25% (ref. 5).

Table 13: *Bucklings and eigenvalues for critical cores*

| Core | Coolant | Buckling ($m^{-2}$) Radial | Buckling ($m^{-2}$) Axial | *k*-eff End fitting correction | *k*-eff METH. II | *k*-eff Random error | *k*-eff WIMS |
|---|---|---|---|---|---|---|---|
| SG11 | Air | 3·26±0·11 | 3·57±0·02 | +0·0128 | 1·0411 | ±0·0028 | |
| SG11 | Water | 5·76±0·13 | 5·58±0·03 | +0·0378 | 0·9895 | ±0·0018 | |
| SG12 | Mixture | 2·55±0·12 | 4·06±0·03 | +0·0117 | 0·9808 | ±0·0026 | |
| SG12 | Water | 2·57±0·04 | 3·68±0·04 | +0·0127 | 0·9765 | ±0·0011 | |
| SG13 | Air | 3·07±0·02 | 2·95±0·02 | +0·0069 | 1·0171 | ±0·0007 | |
| SG13 | Mixture | 3·23±0·01 | 4·64±0·48 | +0·0215 | 0·9972 | ±0·0092 | |
| SG13 | Water | 3·29±0·12 | 6·80±0·30 | +0·0293 | 0·9743 | ±0·0049 | |
| SG14 | Air (voided D.T.'s) | 2·86±0·03 | 2·63±0·05 | +0·0064 | 1·0186 | ±0·0016 | |
| SG14 | Mixture (voided D.T.'s) | 3·10±0·04 | 4·73±0·34 | +0·0210 | 0·9880 | ±0·0067 | |
| SG14 | Water (voided D.T.'s) | 3·17±0·06 | 6·03±0·20 | +0·0281 | 0·9815 | ±0·0033 | |
| SG15 | Mixture (voided D.T.'s) | 2·91±0·03 | 1·28±0·07 | | 0·9934 | ±0·0027 | |
| SG15 | Water (voided D.T.'s) | 2·93±0·02 | 2·35±0·08 | | 0·9899 | ±0·0021 | |
| SG15 | Mixture | 3·16±0·03 | 3·56±0·07 | | 1·0055 | ±0·0019 | 0·9966 |
| SG15 | Water | 3·21±0·03 | 4·51±0·04 | | 1·0037 | ±0·0010 | 0·9899 |
| SG17 | Mixture (0 ppm B10) | 2·97±0·02 | 3·73±0·03 | | 1·0053 | ±0·0007 | 0·9968 |
| SG17 | Mixture (2 ppm B10) | 2·99±0·02 | 2·91±0·02 | | 1·0037 | ±0·0007 | 0·9952 |
| SG17 | Mixture (4·5 ppm B10) | 3·00±0·02 | 2·13±0·01 | | 1·0010 | ±0·0005 | 0·9951 |
| SG19 | Water | 5·67±0·13 | 2·39±0·02 | | 1·0028 | ±0·0024 | 0·9893 |
| SGP1 | Mixture | 5·66±0·06 | 0·52±0·02 | | 1·0015 | ±0·0014 | 1·0025 |
| SGP1 | Water | 5·69±0·07 | 1·28±0·04 | | 1·0012 | ±0·0015 | 0·9982 |
| SGP2 | Mixture | 5·96±0·13 | 2·22±0·02 | | 0·9906 | ±0·0025 | 0·9947 |
| SGP2 | Water | 5·97±0·13 | 3·27±0·025 | | 0·9903 | ±0·0023 | 0·9936 |
| | | | *Average values:* (Excluding SG11–14, see para. 89) | Mixture | 1·0001 | | 0·9968 |
| | | | | Water | 0·9976 | | 0·9928 |

*Note:* The estimated uncertainty in the calculated end plate corrections is ±25% (ref. 5).

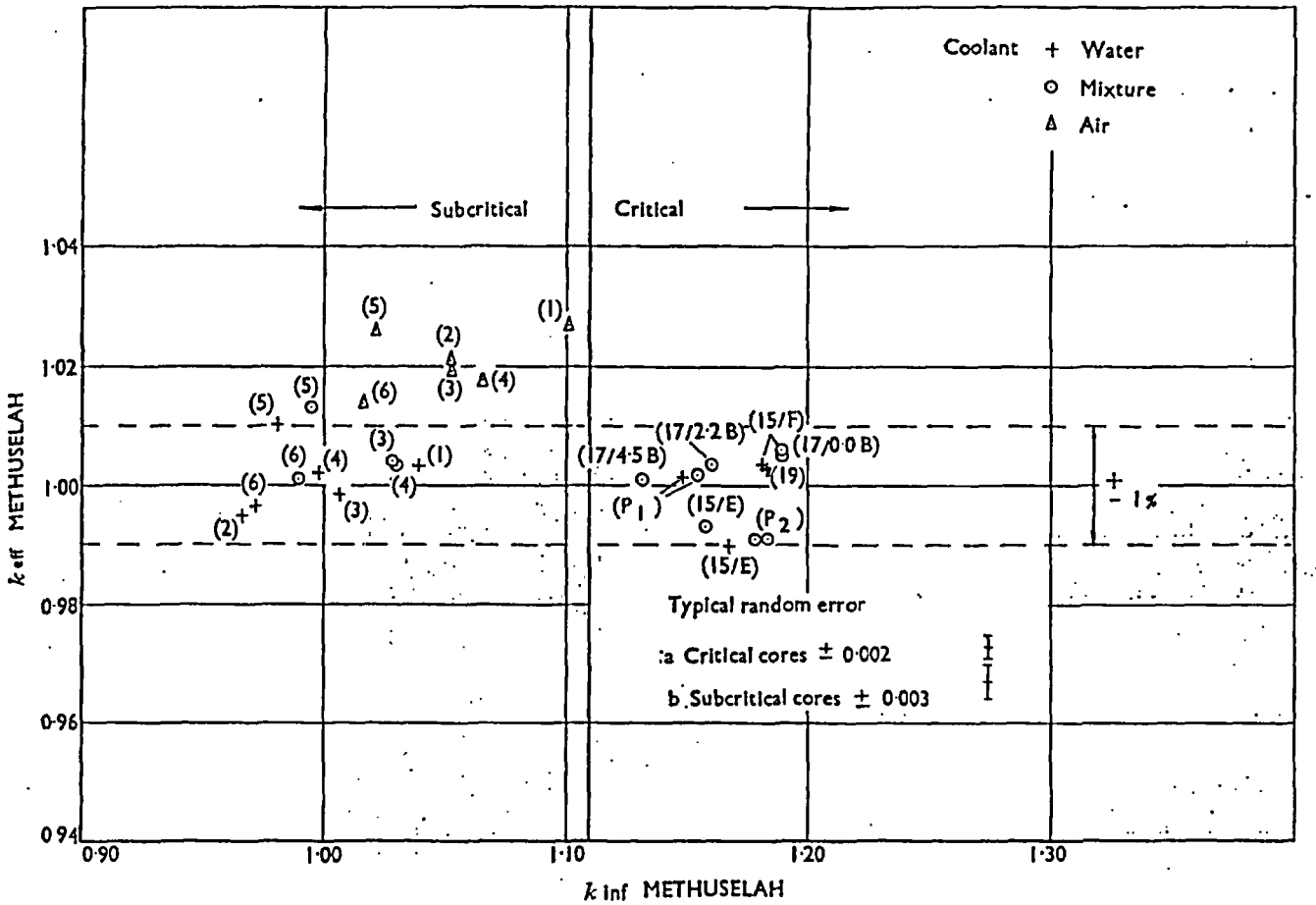


*Fig 14* Variation of *k*-eff with *k*-inf from METHUSELAH

and buckling measurements of limited accuracy only could be obtained. All the eigenvalues for those cores with liquid coolant are low by an average of 1·6%. The end plates in these cores SG11–14 were similar to those in the sub-critical lattices which have relatively good eigenvalues. The leakage in cores SG11–14 was similar to that in the later critical cores SG15 *et seq.*, which use continuous fuel and also have good eigenvalues. It is therefore concluded that the presence of a plane of end plates in the central regions of the early critical cores has given rise to significant systematic errors in the measurements of material buckling as discussed in reference 4, and these cores have therefore been omitted from Fig. 14. Rejecting these cores, the average eigenvalues for the three coolants are as follows:

| *Coolant* | *Effective coolant density* | *METHUSELAH k-effective* |
|---|---|---|
| Water | 1·0 g/cm³ | 0·999 ± 0·006 |
| Mixture | 0·4 to 0·7 g/cm³ | 1·002 ± 0·005 |
| Air | 0·0 g/cm³ | 1·021 ± 0·005 |

90. The elimination of cluster end fittings from core SG15 *et seq.* leads to much less uncertainty in the comparison between theory and experiment, and the relevant figures in Table 13 show that for uranium fuelled cores a consistent tendency to overestimate reactivity by up to 0·5% is observed, except in the cores containing voided moderator displacement tubes at each interstitial lattice position. In the latter cores, reactivity is underestimated by ≈1% which provides strong evidence for an overestimate of the effects of neutron streaming from the tubes which is worth 2–3% in reactivity in these cores. The method of taking account of streaming in the displacement tubes is discussed in reference 15, and considering the approximations involved, such eigenvalue discrepancies are not unexpected. The discrepancy should be smaller by a factor of 4 in the much larger core of the SGHWR prototype.

91. Two further trends are observable in the results from the cores without end fittings:

(i) the SG17 cores show evidence of a small trend with boron content. This may be the result of inadequate computation of the boron absorption due to cross-section uncertainties, or to an overestimate of the flux in the poisoned moderator region. The fine structure comparisons in para. 67 (e.g. see Figs 7 and 8) provide little support for the latter

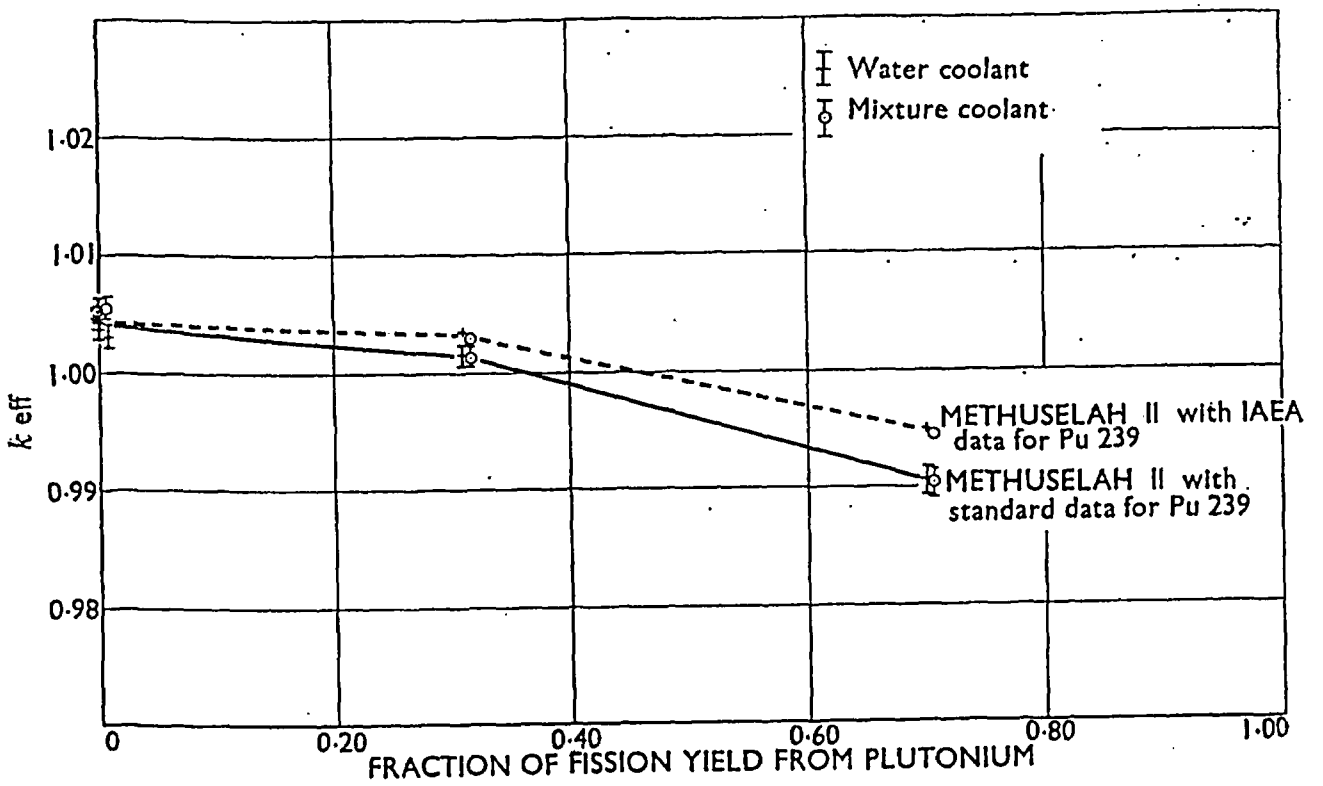


*Fig 15* Variation of METHUSELAH *k*-eff with fraction of fission yield from plutonium

assumption. Alternatively, the eigenvalue trend may be a result of inadequate leakage computations since the cores vary in size with the boron content. However, since this trend represents a reactivity discrepancy of 0·4% in a total reactivity change due to boron of 4%, it is largely of academic interest only;

(ii) the eigenvalues for the SG19, SGP1 and SGP2 cores, which differ in fuel only, decrease as plutonium replaces uranium. These calculations were repeated with the plutonium data in the library changed to give the latest IAEA values[14] of the 2200 m/s cross-sections. This changes the METHUSELAH library value of $\eta_0$ for Pu-239 from the current value of 2·091 to 2·114. No changes were made to the shapes of the fission and absorption cross-sections. A comparison of the two sets of eigenvalues is illustrated in Fig. 15. Although the changes of data are insufficient to remove the trend with fuel composition, the discrepancy between SG19 and SGP2 eigenvalues is reduced from 1·4% to 1·0%.

Table 14: *k-inf in the sub-critical cores*

| | | *k*-inf | | | |
|---|---|---|---|---|---|
| Core | Coolant | Leakage | Reaction rate | *k*-inf (L) −*k*-inf (RR) | METHUSELAH II |
| SG1 | Air | 1·0730 | 1·0868 | −0·0138 | 1·1011 |
| SG1 | Water | 1·0354 | 1·0383 | −0·0029 | 1·0391 |
| SG2 | Air | 1·0307 | 1·0444 | −0·0137 | 1·0516 |
| SG2 | Water | 0·9701 | — | — | 0·9657 |
| SG3 | Air | 1·0305 | 1·0413 | −0·0108 | 1·0505 |
| SG3 | Mixture | 1·0241 | 1·0216 | +0·0025 | 1·0281 |
| SG3 | Beads | — | 1·0140 | — | 1·0189 |
| SG3 | Water | 1·0100 | 0·9999 | +0·0101 | 1·0082 |
| SG4 | Air | 1·0477 | — | — | 1·0652 |
| SG4 | Mixture | 1·0253 | 1·0193 | +0·0060 | 1·0289 |
| SG4 | Water | 0·9971 | 0·9940 | +0·0031 | 0·9995 |
| SG5 | Air | 0·9965 | — | — | 1·0221 |
| SG5 | Mixture | 0·9865 | 0·9958 | −0·0093 | 0·9979 |
| SG5 | Water | 0·9703 | 0·9714 | −0·0011 | 0·9796 |
| SG6 | Air | 0·9983 | — | — | 1·0141 |
| SG6 | Mixture | 0·9882 | 0·9894 | −0·0012 | 0·9895 |
| SG6 | Water | 0·9753 | 0·9654 | +0·0099 | 0·9721 |

92. WIMS estimates of *k*-eff for the later critical cores SG15 *et seq.* are included in Table 13. Values for the earlier cores have not been calculated since the option of WIMS used did not account for end-plates. The overall performance is satisfactory since the discrepancies all lie in the range −1·1% to +0·3%. Uncertainty in basic nuclear data could account for discrepancies of this size. Certain significant trends are observable in these results:

(i) the variation of eigenvalue with concentration of B10 in core SG17 is small, and the trend shown by METHUSELAH is largely eliminated, WIMS predicting a greater reduction in leakage than METHUSELAH;

(ii) there is a tendency for the eigenvalues of the mixture cores to be higher than those of water cores by about 0·7%. This may be linked with a trend observed in the sub-critical cores for WIMS to underestimate RCR by rather more in mixture coolant cores than in water cooled cores. It is believed that a forthcoming revision of the Nuclear Data File for deuterium will remove some of this trend.

### Comparison of $k$-inf (Leakage) and $k$-inf (Reaction Rate)

The reactivity discrepancies can also be expressed by comparing the theoretical $k$-inf values with a $k$-inf (Leakage) obtained from the buckling measurements. The two-group criticality equation gives

$$k\text{-inf} = F\,T\,k\text{-eff} + (1-T)(\eta f)_t(1-p)$$

where

$$F = 1 + B_R^2\,L_{tR}^2 + B_Z^2\,L_{tz}^2$$

$$T = 1 + B_R^2\,L_{tR}^2 + B_Z^2\,L_{tz}^2$$

where subscripts 'f' and 't' refer to fast and thermal neutrons respectively,

$(\eta f)$ is the ratio of fission yield to absorption cross-sections

$p$ is the resonance escape probability

$L_R^2$ is the radial diffusion area, and

$L_Z^2$ is the axial diffusion area.

Table 15: *k-inf in the critical cores*

| Core | Coolant | $k$-inf | | | | |
|---|---|---|---|---|---|---|
| | | Leakage | Reaction rate | $k$-inf (L) $-k$-inf (RR) | METHUSELAH II | WIMS |
| SG11 | Air | 1·2481 | — | — | 1·2996 | |
| SG11 | Water | 1·2411 | — | — | 1·2268 | |
| SG12 | Mixture | 1·1823 | 1·1454 | +0·0369 | 1·1586 | |
| SG12 | Water | 1·1483 | 1·1189 | +0·0294 | 1·1199 | |
| SG13 | Air | 1·1950 | 1·2019 | −0·0069 | 1·2135 | |
| SG13 | Mixture | 1·1941 | 1·1938 | +0·0003 | 1·1899 | |
| SG13 | Water | 1·2119 | 1·1782 | +0·0337 | 1·1792 | |
| SG14 | Air (voided D.T.'s) | 1·1854 | — | — | 1·2062 | |
| SG14 | Mixture (voided D.T.'s) | 1·2014 | — | — | 1·1860 | |
| SG14 | Water (voided D.T.'s) | 1·2014 | — | — | 1·1777 | |
| SG15 | Mixture (voided D.T.'s) | 1·1661 | — | — | 1·1573 | |
| SG15 | Water (voided D.T.'s) | 1·1812 | — | — | 1·1675 | |
| SG15 | Mixture | 1·1838 | — | — | 1·1893 | 1·1889 |
| SG15 | Water | 1·1780 | — | — | 1·1807 | 1·1728 |
| SG17 | (0 ppm B10) | 1·1844 | — | — | 1·1896 | 1·1895 |
| SG17 | (2 ppm B10) | 1·1573 | — | — | 1·1604 | 1·1588 |
| SG17 | (4·5 ppm B10) | 1·1325 | — | — | 1·1325 | 1·1305 |
| SG19 | Water | 1·1801 | 1·1787 | +0·0014 | 1·1817 | 1·1742 |
| SGP1 | Mixture | 1·1567 | — | — | 1·1543 | 1·1641 |
| SGP1 | Water | 1·1494 | — | — | 1·1493 | 1·1529 |
| SGP2 | Mixture | 1·1922 | — | — | 1·1794 | 1·1961 |
| SGP2 | Water | 1·1971 | — | — | 1·1836 | 1·1979 |

Table 16: *Integral void coefficients*

| Core | Effective coolant densities (g/cm³) | | $k$-inf (Leakage) | | Void coefficient $k_v$ | | |
|---|---|---|---|---|---|---|---|
| | Initial ($d_1$) | Final ($d_2$) | Initial ($k_1$) | Final ($k_2$) | Experiment | METHUSELAH | Discrepancy |
| †SG3 | 1·00 | 0·42 | 1·0100 | 1·0305 | +0·025±0·002 | +0·032 | +0·007 |
| SG4 | 1·00 | 0·42 | 0·9971 | 1·0253 | +0·042±0·002 | +0·044 | +0·002 |
| †SG5 | 1·00 | 0·42 | 0·9703 | 0·9865 | +0·029±0·003 | +0·031 | +0·002 |
| †SG6 | 1·00 | 0·42 | 0·9753 | 0·9882 | +0·024±0·006 | +0·030 | +0·006 |
| SG12 | 1·00 | 0·40 | 1·1483 | 1·1823 | +0·038±0·003 | +0·035 | +0·003 |
| SG13 | 1·00 | 0·40 | 1·2119 | 1·1941 | −0·011±0·011 | +0·018 | +0·029 |
| †SG14 | 1·00 | 0·40 | 1·2014 | 1·2014 | 0·000±0·008 | +0·015 | +0·015 |
| †SG15(E) | 1·00 | 0·42 | 1·1812 | 1·1661 | −0·015±0·004 | −0·011 | +0·004 |
| SG15(F) | 1·00 | 0·42 | 1·1780 | 1·1838 | +0·007±0·002 | +0·009 | +0·002 |
| SGP1 | 1·00 | 0·43 | 1·1494 | 1·1567 | +0·006±0·002 | +0·007 | +0·001 |
| SGP2 | 1·00 | 0·57 | 1·1971 | 1·1922 | −0·007±0·005 | −0·006 | +0·001 |
| | | | | | *Average discrepancy* (excluding SG12, 13 and 14) | | +0·003 |

*Notes:* (1) † These cores had empty moderator displacement tubes or an increased gas gap between the pressure and calandria tubes.
(2) The error shown is the random experimental error obtained from errors on the measured bucklings.
(3) The estimated uncertainty in the leakage parameters[5] implies a systematic error of ±0·003.
(4) The estimated uncertainty in the calculated end plate corrections[6] implies a systematic error of ±0·002 on the measurements in cores SG3–SG14 inclusive.[6]

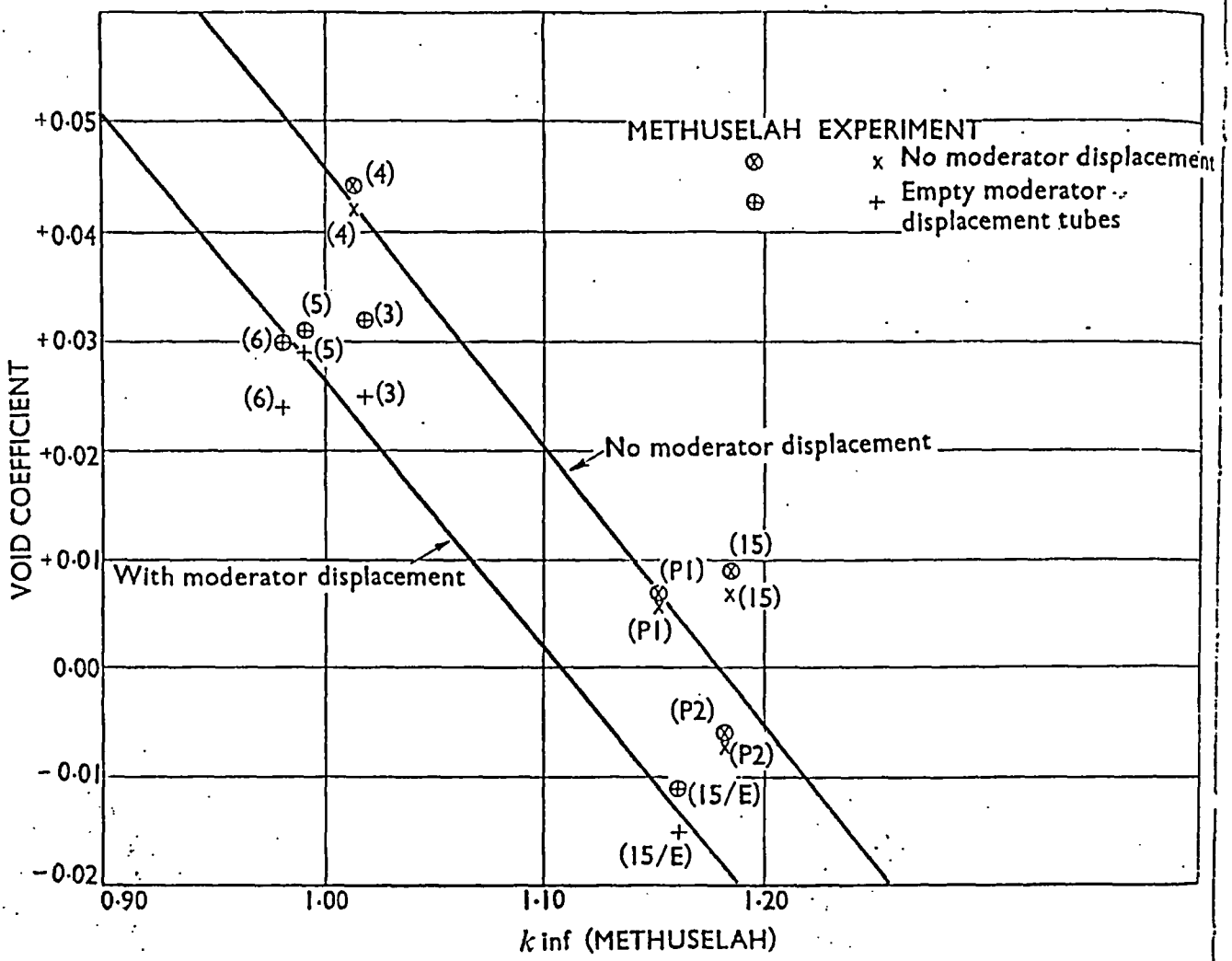


*Fig 16* Void coefficient of *k*-inf

94. Thus *k*-eff can be obtained by using the theoretical *k*-inf, experiment bucklings and theoretical leakage parameters. Alternatively, one can argue that in any static experiment the *k*-eff of the system is unity, and thus use the above equations to determine an experimental *k*-inf (Leakage). It is preferable to work in terms of a lattice without end plates; the expression used for computing *k*-inf (Leakage) is therefore:

$$k\text{-inf(Leakage)} = FT + (1-T)(\eta f)_t(1-p) + k\text{-inf(METHUSELAH, clean)} - k\text{-inf(METHUSELAH, with end plates)}$$

All the parameters were taken from METHUSELAH calculations.

95. An alternative method of obtaining an experimental *k*-infinity is to correct the theoretical value by increments obtained from the various reaction rate discrepancies. The details of the method of computation of *k*-inf (Reaction Rate) are described in reference 20 and the numbers used here are listed in reference 15. Comparisons of the various *k*-inf values are given in Tables 14 and 15.

96. The early critical cores SG11–13, which gave anomalous eigenvalues due to end plate effects near the centre plane of the core, are again seen to give singularly large discrepancies between *k*-inf (RR) and *k*-inf (L). If these cores are omitted, the average discrepancies between *k*-inf (L) and *k*-inf (RR) are as follows:

| *Coolant* | *Discrepancy* |
|---|---|
| Water | $+0{\cdot}0034 \pm 0{\cdot}0055$ |
| Mixture | $-0{\cdot}0005 \pm 0{\cdot}0066$ |
| Air | $-0{\cdot}0127 \pm 0{\cdot}0017$ |

97. Since these values originate in completely independent and different types of measurement, this agreement provides some evidence that for water and mixture cooled areas no significant sources of systematic error are being overlooked. The lack of any trend with the value of *k*-infinity also implies that the calculation of leakage gives results of adequate accuracy for these experimental SGHW lattices.

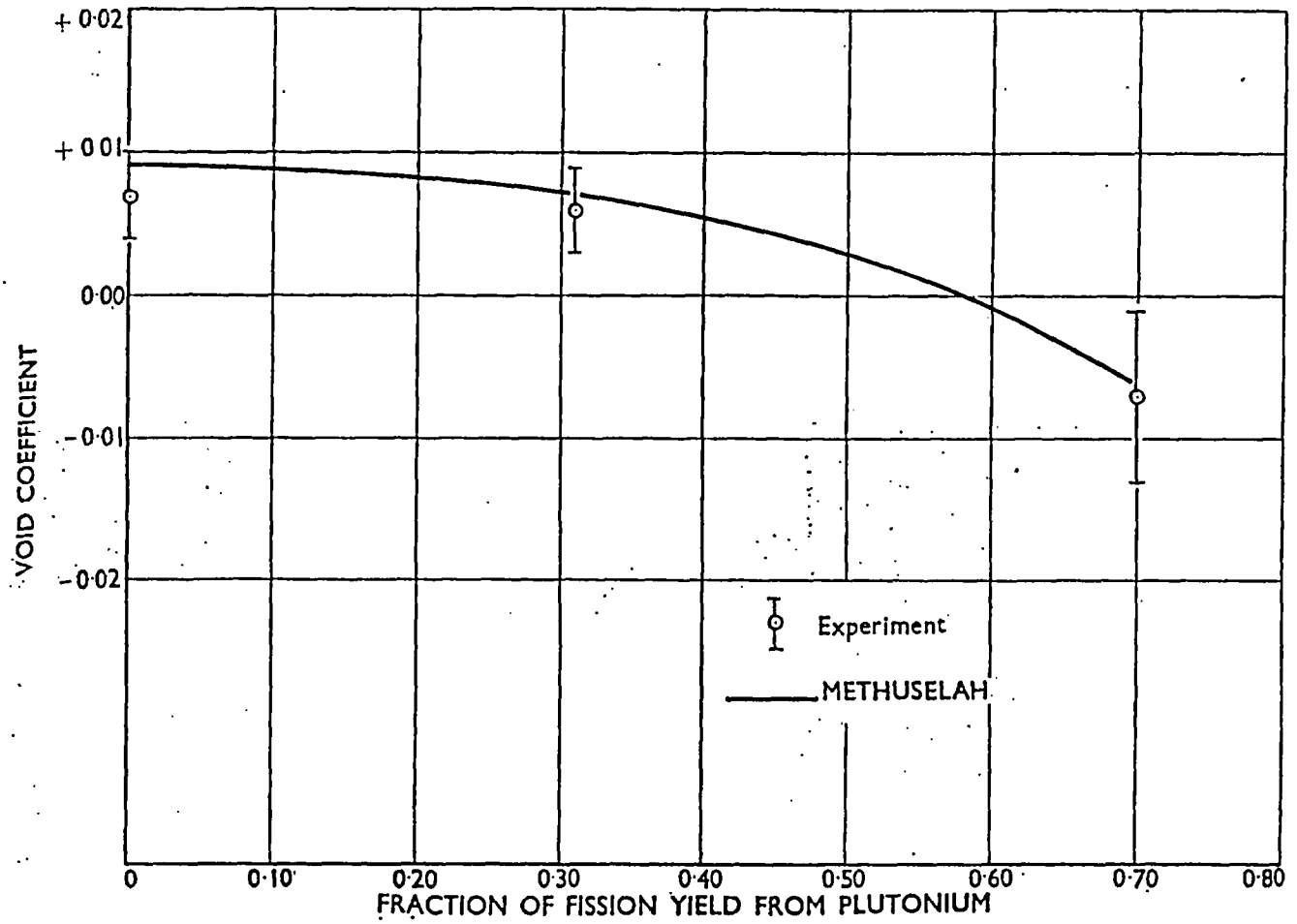


*Fig 17* Variation of void coefficient of $k$-inf with fraction of fissions in plutonium

## INTEGRAL VOID COEFFICIENT

Void coefficients of $k$-infinity have been obtained from the material buckling measurements at different effective coolant densities using calculated leakage parameters as described in reference 4. The results of these integral measurements are compared with METHUSELAH predictions in Table 16. For each core the void coefficient $k_v$ is calculated from the expression

$$k_v = \frac{0{\cdot}72}{(d_1 - d_2)} \frac{(k_1 - k_2)}{\bar{k}}$$

where $d$ is the effective coolant density (see para. 10)

$\bar{k}$ is the mean value of $k$-inf, and

subscripts 1 and 2 denote the initial and final states respectively.

99. The accuracy of the measurements of material buckling was discussed in para. 24. The improved accuracy which was achieved in the later critical measurements with continuous fuel (cores SG15 *et seq.*) is reflected in the improved determinations of void coefficient in these cores as shown in Table 16. For the purposes of estimating the probable error in the measured void coefficient, an uncertainty of ±2% has been assigned to the change in axial migration area with coolant density and ±4% to the corresponding change in radial migration area as discussed in reference 5.

100. These results are illustrated in Fig. 17, the measurements with larger uncertainties due to cluster end effects in the early critical cores SG11–14 being omitted. The following trends are observed:

(i) METHUSELAH overestimates the void coefficient in every uranium fuelled core by an average of 0·004;

(ii) the void coefficient becomes significantly more positive as the fuel enrichment is reduced due to the increased importance of parasitic neutron absorption in the coolant;

(iii) the presence of empty moderator displacement tubes (or an equivalent increase in the gas gap) makes the void coefficient more negative by about 0·02;

(iv) the successive replacement of uranium by plutonium in clusters of identical geometry (SG15—SGP1—SGP2) until 70% of the fissions take place in plutonium, makes the void coefficient more negative by $0{\cdot}014 \pm 0{\cdot}005$. This effect is due mainly to the higher absorption cross-section of plutonium decreasing the relative importance of parasitic absorption. The trend is well predicted by METHUSELAH as illustrated in Fig. 17, even though it was shown in para. 85 that errors in the prediction of thermal spectrum effects should introduce an error of $+0{\cdot}006$ in the METHUSELAH prediction of void coefficient in core SGP2.

## CONCLUSIONS

The METHUSELAH II and WIMS methods of calculation have been tested over a wide range of SGHW lattices with uniform cluster geometry. The main results are as follows:

(i) Fast fission ratio (FR)

The renormalization of the U-238 fast data in METHUSELAH to SPEC Monte Carlo calculations has led to a considerable improvement in the prediction of fast fission ratio, the average discrepancy for liquid cooled cores being 0·4%. However, WIMS shows a consistent tendency to underestimate the measured fission ratio by 10%, which is comparable with some previous comparisons of WIMS, with undermoderated uniform $UO_2$–$H_2O$ lattices (e.g. reference 35). A careful comparison of the WIMS calculations with SPECIFIC Monte Carlo calculations and an evaluation of uncertainties in current fast data imply that an underestimate of this magnitude is unlikely, and the possibility of an unsuspected systematic error in the measured fission ratio cannot therefore be ruled out. Further measurements by an alternative technique are planned to provide additional evidence on this point.

103. The rise in the measured fission ratio towards the centre of the cluster is overestimated by METHUSELAH and also by WIMS but to a lesser extent. Since both methods of calculation predict the thermal flux distribution in the cluster well, these discrepancies in the FR distribution are largely associated with the predictions of fast events.

(ii) Relative conversion ratio (RCR)

METHUSELAH predictions based on Hellstrand's measurements of resonance integral for single rods,[29] and WIMS calculations using resonance cross-sections from the UKAEA Nuclear Data File[30] reduced as proposed by Askew[31] both give relatively good agreement with the measured RCR values which are believed to be free from systematic errors greater than ±1%. For the liquid cooled clusters, METHUSELAH underestimates RCR by an average of 0·7%, while WIMS underestimates water cooled cores by 1·5% and mixture cooled cores by 3·5%. Revisions to the Nuclear Data File for deuterium are expected to improve these predictions, but the residual errors suggest that a rather smaller correction to U-238 data than that proposed by Askew is required for these cores.

105. The cluster distributions show the same trends as were observed in the FR comparison, METHUSELAH tending to overestimate the increase in RCR near the centre of the cluster, while the WIMS results are much closer to the experimental values.

(iii) Thermal fine structure

METHUSELAH gives satisfactory predictions of maximum/average reaction rate ratios in liquid cooled clusters, the average discrepancies being $+2{\cdot}2 \pm 2{\cdot}3\%$ for mixture coolant and $+3{\cdot}2 \pm 3{\cdot}2\%$ for water coolant. In the SG1, SG13 and subsequent cores, which used fairly uniform multi-rod clusters, METHUSELAH predictions of maximum/average ratios are very consistent being high by $4 \pm 1\%$ for mixture coolant and by $5 \pm 1\%$ for water coolant. The WIMS predictions are similarly good, averaging $+1{\cdot}3 \pm 1{\cdot}1\%$ and $+3{\cdot}0 \pm 2{\cdot}0\%$ for mixture and water coolants respectively. Some measurements have also been made on the pressure and calandria tubes, in the $D_2O$ bulk moderator, and on moderator displacement tubes at interstitial lattice positions. For liquid cooled cores, METHUSELAH generally predicts this fine structure to better than ±5%, with rather larger discrepancies for air cores. There is a slight trend for METHUSELAH to overestimate the increase in fine structure with coolant density in uranium fuelled cores. WIMS predictions of the thermal fine structure across the cell are in good agreement with experiment both for liquid and air coolants.

(iv) Thermal hyperfine structure. (Disadvantage factor)

Measurements of thermal disadvantage factor have been made with 0·005 in. manganese–nickel foil in seven of the cores studied. Both METHUSELAH and WIMS predict the observed values within about ±2% which is comparable with the quoted experimental errors.

(v) Integral thermal spectrum

The use of a gas model for $H_2O$ in METHUSELAH leads to a consistent tendency to predict too soft a spectrum and hence to underestimate the plutonium/uranium and lutecium/manganese ratios in the centre of the clusters, although this is counterbalanced to some extent by a tendency to underestimate the change in spectrum across the cluster. For liquid fuelled clusters the average discrepancies are $+0{\cdot}3\%$ for the plutonium/uranium ratio and $-5{\cdot}6\%$ for the lutecium/manganese ratio. The WIMS calculations presented in this Paper use the Nelkin and Honeck models for light and heavy water respectively, resulting in a marked improvement particularly in the predictions of lutecium/manganese reaction rate ratios. The average discrepancies with experiment in the liquid cooled clusters were $+0{\cdot}3\%$ for the plutonium/uranium ratio and $+0{\cdot}3\%$ for the lutecium/manganese ratio. Even in a plutonium fuelled system, the reactivity is relatively insensitive to the detailed shape of the thermal neutron spectrum, and hence the METHUSELAH predictions of thermal spectrum are clearly adequate for reactor design purposes as shown by its excellent performance in predicting reactivity and void coefficients in these SGHW lattices.

109. The more detailed treatment of thermal neutron spectra available in WIMS has been used to study the distribution of integral neutron spectrum across typical SGHW clusters, and it has been shown to give good agreement with the experiments, whereas METHUSELAH predicts too flat a distribution, particularly in the case of the plutonium/uranium ratio.

110. The variation of integral thermal neutron spectrum with effective coolant density is a particularly interest-

ing phenomenon. As moderator is removed in a uranium fuelled system, the spectrum hardening increases both the plutonium/uranium and lutecium/manganese ratios. When a considerable proportion of plutonium is present in the lattice, however, the flux in the vicinity of the 0·3 eV resonance in plutonium is depressed and the effect of moderator removal is to increase the importance of the effect and hence to decrease the plutonium/uranium and lutecium/manganese ratios. The experimental measurements in a series of three cores of identical geometries but different plutonium content are compared with METHUSELAH and WIMS predictions in Figs 12 and 13. Neither of the theoretical methods is found adequate to describe the observed trends in detail but the WIMS predictions are, as expected, rather better than the METHUSELAH predictions. In each case METHUSELAH underestimates the change of spectrum with coolant density. The reactivity worth of the discrepancy is small for a uranium fuelled core, but in the plutonium fuelled core SGP2 the discrepancy implies an error in calculation of the void coefficient of +0·006.

(vi) Eigenvalues

Comparison of measured bucklings with METHUSELAH indicates that reactivity is being calculated to within ±1% over a wide range of liquid cooled cores. The improved treatment of air cores available in METHUSELAH II has reduced the overestimate of reactivity in air cores to 2%. The accuracy of the measurements allowed three further small trends to be identified. Firstly, there is evidence that the leakage from cores containing empty moderator displacement tubes is being overestimated. This is of little significance for reactor design because of the relative unimportance of leakage in a large power reactor. Secondly, the reactivity worth of dissolving boron in the moderator is slightly overestimated. Thirdly, there is evidence of a slight tendency for the predicted reactivity to be lower in the cores containing a substantial fraction of plutonium. Even without making allowances for these effects, METHUSELAH predicts reactivity to within 1%; if allowance is made for these trends it is possible to predict the reactivity of enriched SGHW cores to better than 0·5%. For a small number of critical cores, WIMS calculates the reactivity to within ±1%. In WIMS there is a tendency for mixture cooled cores to be slightly more reactive than water cooled cores, which is probably associated with the tendency to underestimate RCR in mixture cores.

(vii) Comparison of *k*-inf (Leakage) and *k*-inf (Reaction Rate)

Comparison of values of *k*-inf deduced from measured bucklings, *k*-inf (L), with values deduced from measured reaction rates, *k*-inf (RR), does not show any systematic discrepancy for liquid cooled cores. Since these measurements are independent, this provides some evidence that the experimental estimates of *k*-inf are free from significant systematic errors.

(viii) Void coefficient

METHUSELAH calculations of void coefficient have been shown to be remarkably accurate over the range of cores studied. The mean discrepancy for uranium fuelled cores was +0·004 while for the plutonium fuelled cores the discrepancy was even lower. This result is consistent within the minimum total experimental uncertainty of ±0·005 (see Table 16) with the conclusion from reactivity measurements reported elsewhere[45] that the mean error in the prediction of the void coefficient of reactivity is small. Although the METHUSELAH prediction of void coefficients may involve some small cancellation of errors, the success of the code over the range of experimental cores provides strong confirmation that the void coefficient is calculated well within the accuracy required for reactor design.

## GENERAL CONCLUSION

This comparison has shown that METHUSELAH predictions of reactivity, void coefficient and power peaking are in excellent agreement with experiment, confirming its accuracy for the design and assessment of enriched SGHW cores. A discrepancy between WIMS and measured Fast Ratios is of general interest but is of relatively little importance for SGHW calculations, and the improved predictions available from WIMS for cluster distributions and spectral effects, make it a particularly useful tool for the investigation of special effects in SGHW reactors.

## ACKNOWLEDGEMENTS

The experimental work described in this Paper has been carried out by many members of Water Reactor Physics Division, and their help is gratefully acknowledged. Thanks are also due to Dr C. G. Campbell who was in overall charge of this work, for much helpful advice during the programme, and to Low Power Reactor Operations Group of General Operations and Technology Division, for their willing co-operation and efficient operation of the experimental plant.

## REFERENCES

1. Firth A. and Holmes J. E. R. The SGHW prototype reactor. *Nucl. Engng* 1964, 9, 46
2. Cartwright H. SGHWR—A dark horse competitor. *Nucleonics* 1966, 24 (9), 60
3. Campbell C. G., Hicks D., Johnstone I. and Leslie D. C. Reactor physics studies for steam generating heavy water reactors. *Proc. 3rd Int. Conf. on the Peaceful Uses of Atomic Energy, Geneva*, 1964, P174
4. Campbell C. G., Johnstone I., Leslie D. C. and Newmarch D. A. Reactor physics studies for steam generating heavy water reactors—A comparison of experimental results with theoretical predictions. AEEW-R336
5. Campbell C. G. and Johnstone I. The experimental basis of reactor physics predictions for cold, clean SGHW lattices. AEEW-R337
6. Fox W. N., Goddard A. J. H. and Wells G. M. Measurements of thermal neutron flux peaking in SGHW lattices. AEEW-R339
7. Brown W. A. V. and Skillings D. J. The measurement of relative conversion ratio in low enrichment oxide lattices. AEEW-R340
8. Brown W. A. V. and Skillings D. J. Measurement of fast fission ratio. AEEW-R341
9. Fox W. N. Characterisation of thermal spectra by integral techniques. AEEW-R342
10. Goddard A. J. H. and Johnstone I. Measurement of material buckling in a large heterogeneous exponential assembly. AEEW-R352

11. ALPIAR R. METHUSELAH. A universal assessment programme for liquid moderated reactors using IBM 7090 or STRETCH. AEEW-R135
12. LESLIE D. C. and TERRY M. J. A preliminary description of THULE. AEEW-R250
13. BRINKWORTH M. J. and GRIFFITHS J. A. METHUSELAH II—A Fortran program and Nuclear Data Library for the physics assessment of liquid-moderated reactors. AEEW-R480
14. ASKEW J. R., FAYERS F. J. and KEMSHELL P. B. A general description of the lattice code WIMS. *J. Brit. Nucl. Energy Soc.* 1966, 5, 564
15. BRIGGS A. J., JOHNSTONE I., KENDALL K. C. and NEWMARCH D. A. Further reactor physics studies for steam generating heavy water reactors. Part 1. Uniform cluster lattices containing $UO_2$ or $PuO_2/UO_2$ fuel. AEEW-R548
16. KEMSHELL P. B. and NEWMARCH D. A. An analysis of heavy water moderated cluster lattices using the WIMS code. AEEW-R549
17. GODDARD A. J. H. and MADDISON R. J. The SGHW I experiment at AEE Winfrith. Part 1: Description of the plant, and details of the lattice studied. AEEW-R338
18. BARNETT G. A., BROWN W. A. V. and FERRETT D. J. The separation and precise determination of 239 neptunium in irradiated low enrichment uranium oxide foils and pellets. AEEW-R202, 1964
19. BENOIST P. Formulation générale et calcul pratique du coéfficient de diffusion dans un réseau comportant des cavités. CEA 1354
20. NEWMARCH D. A. A method of inferring *k*-infinity from reaction rate measurements in thermal reactor systems. AEEW-R512
21. BROOMFIELD A. M. and STEVENSON J. M. Measurements and calculations of ratios of effective fission cross-sections in the zero-power fast reactor ZEBRA. AEEW-R526
22. SMITH R. D. ZEBRA—A zero power fast reactor. *Nucl. Engng* 1962, 7 (76), 346
23. TAYLOR W. H., MURPHY M. F. and SMITH G. Experimental investigation of foil edge effects in relative conversion ratio (RCR) measurements. ETM/P68. (Private communication)
24. TAYLOR W. H. and MURPHY M. F. Experimental investigation of foil edge effects in RCR measurements. ETM/P73. (Private communication)
25. BANNISTER G. W., BASHER J. C. and PULL I. C. MOCUP—A Monte Carlo programme for estimating resonance escape in complex geometries. AEEW-R243
26. NEWMARCH D. A. RIPPLE—A method of computing the thermal neutron fine structure for thin plate assemblies. AERE—R/R 2425
27. LESLIE D. C. The calculation of removal cross-sections between overlapping thermal groups AEEW-R133
28. FRANCESCON S. A Monte Carlo programme for calculating high energy spectra in cylindrical geometry for the IBM 709 computer. AEEW-R45, 1960
29. HELLSTRAND E. Measurements of resonance integrals. Reactor physics in the resonance and thermal regions. *Proc. ANS Topical Meeting, San Diego*, 1966. Massachusetts Institute of Technology, Cambridge, Massachusetts, 1966, vol. 2, p. 151
30. HELLSTRAND E. Measurements of the effective resonance integral in uranium metal and oxide in different geometries. *J. Appl. Phys.* 1957, 28, 1493
31. KENDALL K. C. and TERRY M. J. NOAH—A modified output scheme for METHUSELAH for experimental analysis. AEEW-M756
32. BUCKLER A. N. and MACDOUGAL J. D. A description of the TRACER-1 computational scheme. AEEW-R305, 1963
33. ASKEW J. R., FAYERS F. J. and KEMSHELL P. B. A general description of the lattice code WIMS. *J. Brit. Nucl. Energy Soc.* 1966, 5, 564
34. FAYERS F. J., KEMSHELL P. B. and TERRY M. J. An evaluation of some uncertainties in the comparison of theory and experiment for regular light water lattices. *J. Brit. Nucl. Energy Soc.* 1967, 6, 161
35. FAYERS F. J. and KINCHIN G. H. Uranium and plutonium fuelled lattices with graphite and water moderation—A comparison of experiment and theory. *Proc. Conference on Physics Problems in Thermal Reactor Design*, June 1967, Paper 1. British Nuclear Energy Society, London, 1967
36. STORY J. S., KERR W. M. M., PARKER K., PULL I. C. and SCHOFIELD P. Evaluation, storage and processing of nuclear data for reactor calculations. *Proc. 3rd Int. Conf. on the Peaceful Uses of Atomic Energy, Geneva*, 1964, P168
37. BELL V. J. *et al.* A users guide to GALAXY 3. AEEW-R379, 1964
38. BRISSENDEN R. J. and DURSTON C. The calculation of neutron spectra in the Doppler region. Conference on the Application of Computing Methods to Reactor Problems. ANL 7050, p. 51, 1965
39. LESLIE D. C. The 'Spectrox' method for thermal spectra in lattice cells. *J. Nucl. Energy*, 1963, 17, 293
40. BEARDWOOD J. E., CLAYTON A. J. and PULL I. C. The solution of the transport equation by collision probability methods. Conference on the Application of Computing Methods to Reactor Problems. ANL 7050, pp. 93–110, 1965
41. RUFFLE M. P. SPECIFIC—A Monte Carlo programme for high energy spectrum estimation. AERE-4553, 1964
42. BURHOLT G. D. and FOX W. N. A measurement of the microscopic variation of manganese reaction rate in SGHW type clusters. (Private communication)
43. NEWMARCH D. A. A theoretical interpretation of the pressure-tube, heavy water, zero energy experiment in DIMPLE. Technical Reports Series, No. 20. International Atomic Energy Agency, Vienna 1963
44. WESTCOTT C. H. *et al. Atomic Energy Rev.* 1965, 3, 3–60